ANALYSIS OF PCG SIGNAL TO CLASSIFY VARIOUS HEART DISEASES

A Dissertation submitted in fulfillment of the requirements for the Degree
of

MASTER OF ENGINEERING
in
Electronics Instrumentation & Control Engineering

Submitted by

Simarjot Kaur Randhawa
801351027

Under the Guidance of
Dr. M.D. Singh
Assistant Professor, EIED

2015

Electrical and Instrumentation Engineering Department
Thapar University, Patiala
(Declared as Deemed-to-be-University u/s 3 of the UGC Act., 1956)
Post Bag No. 32, Patiala – 147004
Punjab (India)

DECLARATION

I hereby certify that the work which is presented in dissertation entitled, "**Analysis of PCG Signal to Classify Various Heart Diseases**" in partial fulfillment of the requirements for the award of the degree of **Master of Engineering** in **Electronics (Instrumentation & Control)**, submitted to Electrical & Instrumentation Engineering Department of Thapar University, Patiala is as authentic record of my own work carried under the supervision of **Dr. M.D. Singh**, Assistant Professor, Electrical and Instrumentation Engineering Department, Thapar University, Patiala, Punjab. It refers others researcher's work which are duly listed in the reference section. The matter contained in this dissertation has not been submitted, neither in part nor in full to any other degree to any other university or institute except as reported in text and references.

Simarjot kaur.

Place: Patiala **(Simarjot Kaur Randhawa)**

Date: 15-7-15 Roll No: 801351027

It is certified that the above statement made by the student is correct to the best of my knowledge and belief.

(Dr. MD. Singh)

Assistant Professor

Date: 15/7/15

Electrical & Instrumentation Engineering Department

Thapar University, Patiala

Countersigned by:

Head
Electrical & Instrumentation Engineering Department
Thapar University, Patiala

Dean (Academic Affairs)
Thapar University, Patiala

i

ACKNOWLEDGEMENT

First of all, I would like to express my gratitude to **Dr. M.D. Singh, Assistant Professor**, Electrical and Instrumentation Engineering Department (EIED), Thapar University, Patiala for his patient guidance and support. I am truly very fortunate to have the opportunity to work with him. I found his guidance to be extremely valuable.

I am also thankful to our **Head of the Department, Dr. Ravinder Aggarwal** as well as **PG Coordinator, Mr. Nirbhowjap Singh, Assistant Professor**, Electrical and Instrumentation Engineering Department.

I am extremely thankful to **Dr. Gurmeet Singh, Medical Officer**, Civil Hospital, Ludhiana for his helpful guidance the time he devoted on me to help me to understand the medical concepts more clearly.

I would like to thank entire faculty and staff of Electrical and Instrumentation Engineering Department and then my friends who devoted their valuable time and helped me in all possible ways towards successful completion of this work. I thank all those who have contributed directly or indirectly to this work.

Lastly, I would also like to thank my parents for their years of unyielding love and encourage. They have always wanted the best for me and I admire their determination and sacrifice.

Date: 15-7-15

Place: Patiala

Simarjot Kaur Randhawa

M.E. (EICE) 2nd Year

801351027

ii

TABLE OF CONTENTS

Contents **Page No.**

Contents		Page No.
DECLARATION		i
ACKNOWLEDGEMENT		ii
LIST OF TABLES		v
LIST OF FIGURES		vi
LIST OF ABBREVIATIONS		viii
ABSTRACT		ix
CHAPTER 1	**INTRODUCTION**	**1-7**
	1.1 Overview	1
	1.2 Phonocardiography	2
	1.3 Aim of Work	4
	1.4 Outline of Thesis	6
CHAPTER 2	**THE HEART**	**8-19**
	2.1 Importance of the Heart	8
	2.2 Anatomy	8
	2.2.1 Pericardium	8
	2.2.2 Chambers of the Heart	9
	2.2.3 Valves of the Heart	10
	2.2.4 Conduction System of the Heart	11
	2.3 Physiology	12
	2.3.1 Normal Physiology	12
	2.3.2 Abnormal Physiology	14
	2.4 Heart Sounds	15
	2.4.1 Normal Heart Sounds	15
	2.4.2 Abnormal Heart Sounds	16
CHAPTER 3	**LITERATURE REVIEW**	**20-28**
CHAPTER 4	**MATERIALS AND METHODOLOGY**	**29-39**
	4.1 Materials used	29
	4.2 Methodology	29

	4.2.1 Signal Acquisition	30
	4.2.2 Feature Extraction	30
	4.2.3 Feature Reduction	34
	4.2.4 Classification	36
	4.3 Algorithm for Adaptive Weighted Fisher Discriminant Ratio	37
CHAPTER 5	**RESULTS**	**40-70**
	5.1 Feature Evaluation	40
	5.2 Classification of Signals Using Different Classifiers	43
	5.2.1 Feature Extraction	43
	5.2.2 Feature Reduction	62
	5.2.3 Classification	63
	5.3 Classification of PCG signals using Adaptive Weighted FDR Algorithm	69
CHAPTER 6	**CONCLUSION AND FUTURE SCOPE**	**73**
	6.1 Conclusion	73
	6.2 Future Scope	73
REFERENCES		**74-79**
LIST OF PUBLICATIONS		**80**
PLAGIARISM CERTIFICATE		

LIST OF TABLES

Table No.	Caption	Page
3.1	Comparison table of different methodologies used in various studies	26
4.1	List of features that were extracted for classification	34
5.1	Time domain features of normal signals	43
5.2	Features extracted in systolic and diastolic regions of normal signals	45
5.3	Frequency domain features of normal signal	47
5.4	Statistical domain features of normal signals	49
5.5	Time domain features of diastolic signals	51
5.6	Features extracted in systolic and diastolic regions of diastolic murmur signals	52
5.7	Frequency domain features of diastolic murmur signal	54
5.8	Statistical domain features of diastolic murmur signals	55
5.9	Time domain features of systolic murmur signals	57
5.10	Features extracted in systolic and diastolic regions of systolic murmur signals	58
5.11	Frequency domain features of systolic murmur signal	59
5.12	Statistical domain features of systolic murmur signals	60
5.13	Value of FDR ratio calculated for each feature	62
5.14	List of features that were selected for classification.	63
5.15	Accuracies using k-NN as a classifier	66
5.16	Accuracies using Fuzzy k-NN as a classifier	68
5.17	Selected features and their FDR weight value	69

LIST OF FIGURES

Figure No.	Caption	Page
1.1	Causes of PCG signal generation	2
1.2	A normal PCG signal showing S1 and S2 heart components	3
1.3	A normal PCG signal showing fundamental heart components (FHS)	5
1.4	PCG signal with systolic murmur	5
1.5	PCG signal with diastolic murmur	5
2.1	The Human Heart	10
2.2	Electrical signals coming from Sinoatrial node (SA)	12
2.3	Cardiac Cycle of the Heart	14
2.4	Production of Fundamental Heart Sounds	16
2.5	Systolic and Diastolic murmurs	17
2.6	One of the causes of murmurs i.e. Ventricular Septal Defect (VSD)	18
2.7	Clicks and murmurs in a heart signal	19
4.1	Different stages of the methodology used	30
4.2	Figure showing Ta and Tb in systolic murmur signal	32
4.3	Figure showing Ta and Tb in diastolic murmur signal	32
4.4	A simple multi layer Artificial Neural Network	36
4.5	Classification by kNN classifier	37
4.6	The value of feature lying in the range of value	38
5.1	Plot between Tb and RMS1	41

Figure No.	Caption	Page
5.2	Plot between Tb and Max1	41
5.3	Plot between RMS1 and RMS2	42
5.4	Plot between Max1 and RMS2	42
5.5	Confusion matrix for ANN as a classifier with 5 neurons in hidden layer (Result 1)	64
5.6	Confusion matrix for ANN as a classifier with 5 neurons in hidden layer (Result 2)	64
5.7	Confusion matrix for ANN as a classifier with 5 neurons in hidden layer (Result 3)	65
5.8	Confusion matrix for ANN as a classifier with 5 neurons in hidden layer (Result 4)	65
5.9	Confusion matrix for ANN as a classifier with 5 neurons in hidden layer (Result 5)	66
5.10	5 fold validation and average accuracy using k-NN as a classifier	67
5.11	Average accuracy for different values of k using k-NN as a classifier	67
5.12	5 fold validation and average accuracy using k-NN as a classifier	68
5.13	Average accuracy for different values of k using Fuzzy k-NN as a classifier	69
5.14	Classification of Diastolic murmur signal	70
5.15	Classification of Normal signal	71
5.16	Classification of Systolic murmur signal	71
5.17	Confusion matrix for classification using Adaptive weighted FDR algorithm	72

LIST OF ABBREVIATIONS

ANN- Artificial Neural Network

AR- Aortic Regurgitation

AS- Aortic Stenosis

ASD- Atrial Septal Defect

AV node - Atrioventricular Node

DSP - Digital Subtraction Phonocardiography

DWT- Discrete Wavelet Transform

ECG - Electrocardiography

FDR- Fisher Discriminant Ratio

FFT- Fast Fourier Transform

FHS - Fundamental Heart Sounds

IMD- Intermodulation Distortion

kNN- k Nearest Neighbour

LA - Left Atrium

LV - Left Ventricle

MLP- Multilayer Perceptron

MR- Mitral Regurgitation

MS- Mitral Stenosis

PCG - Phonocardiography

PR- Pulmonic Regurgitation

PS- Pulmonic Stenosis

PWT- Packet Wavelet Transform

RA - Right Atrium

RMS- Root Mean Square

RV - Right Ventricle

SA node – Sinoatrial Node

SVM- Support Vector Machine

THD- Total Harmonic Distortion

VSD- Ventricular Septal Defect

ZCR- Zero Crossing Rate

ABSTRACT

Cardiac auscultation is a technique of listening to heart sounds. Any abnormality in the heart sound may indicate some problem in the heart. The abnormality in the heart sounds start appearing much earlier than the symptoms of the disease start showing. The phonocardiogram (PCG) signal is mainly recorded using an electronic stethoscope. In this study, the PCG signal i.e. the digital recording of the heart sounds has been studied and classified into three classes namely normal signal, systolic murmur signal and diastolic murmur signal. Various features have been extracted for the classification. The features extracted have been plotted against each feature to evaluate the features. It is seen that in some of the plots the three classes were completely separated. A total of 28 features have been extracted and then reduced to 7 features. The features have been selected on the basis of fisher discriminant ratio (FDR) feature reduction technique. The selected features are used to classify the signal into the pre-defined classes using various classifiers. The classifiers which have been used in this study were k-NN (k Nearest Neighbour), fuzzy k-NN and Artificial Neural Network (ANN). Highest accuracy of 99.6% is achieved using both k-NN and fuzzy k-NN as classifiers. Two new features have also been proposed for classification. Also, adaptive weighted FDR algorithm has also been developed to classify the signals. An accuracy of 96% is achieved using this algorithm.

CHAPTER 1

INTRODUCTION

1.1 Overview

In today's world heart diseases are one of the leading causes of human fatality. Heart diseases mainly occur due to the unhealthy lifestyle adopted by the people. Due to heart diseases, the heart sounds may appear abnormal when listened by an experienced doctor with the help of stethoscope. Even in early days doctors used to listen to heart sounds by placing their ears on patients' chest or body. The word 'auscultation' is derived from Latin word 'auscultare' which means 'to listen'. So, we can define auscultation as the act of listening to internal sounds of the body mainly with the help of a stethoscope. Therefore, an act of listening to heart sounds is called cardiac auscultation. The graphic recording of heart sounds is known as phonocardiogram (PCG). Cardiac auscultation is the basic analysis tool which can be used to evaluate the function of the heart [1]. Cardiac auscultation can be used as primary detection technique for detecting heart disorders. The abnormalities in the heart sounds start appearing at an earlier stage of the heart disease before the symptoms start appearing. The main cause of the generation of heart sounds is blood turbulence. The blood turbulence is mainly caused due to opening and closing of heart valves and also due to fast accelerations and retardations of blood flow in the heart chambers [2]. The duration, pitch, shape etc of heart sounds tells or indicates us about the different conditions of the heart. Sometimes unusual sounds appear in the heart sounds which are called murmurs and may indicate some abnormalities in the heart. So, by listening to heart sounds we can diagnose the possibility of developing heart disease and can further analyze the problem using other techniques like Echocardiography and Electrocardiography (ECG) etc and an in-depth study of the problem can be done. This method can also be implemented for infants where it is impossible or difficult to perform ECG. Also, phonocardiography is operationally simple, relatively cheaper technique in comparison with ECG etc and doesn't require much equipment. Therefore, this technique can be used in homecare and primary healthcare set-ups. It can also be used in rural areas where techniques like echocardiography and ECG are not available and the heart health can be monitored by listening to heart sounds. Human errors may be there while diagnosing through heart sounds due to the subjectivity. Therefore, computer based analysis of heart sounds could be a better method for the same. The technique which is proposed in this study is to classify the heart sounds. This technique is just an earlier indicator of the heart problems and not a replacement for the already existing techniques.

1.2 Phonocardiography

The word '*phono*' means sound and has Greek origin. The word '*cardio*' has been derived from Greek word, kardia, which means the heart. The word '*graphy*' means the process of writing and has French origin. So, we can define '*Phonocardiography*' as the process of writing or recording heart sounds. The graphic recording of heart sounds is known as phonocardiogram (PCG). PCG signal is generated due to mechanical activity of heart, blood flow, vibration of chamber valves, opening and closing of valves.

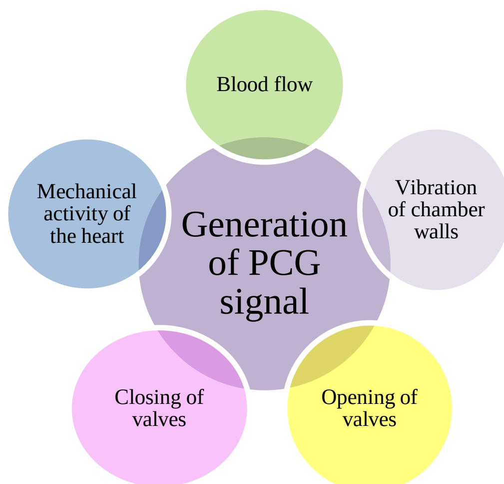

Figure 1.1: Causes of PCG signal generation

It is mainly recorded using electronic stethoscope and the signal is displayed on the computer screen. The heart sounds usually occur at the time of closure of major heart valves. With each heart beat, normal heart produces two distinct sounds- often described as 'lub-dub' [3]. The first heart sound (lub), also known as S1, is caused by the closure of atrioventricular valves. When the blood from atria flows to ventricles, these valves allow unidirectional blood flow i.e. from atria to ventricles and block the reverse blood flow back to atria from ventricles. The second heart sound (dub), also known as S2, is caused due to closure of semilunar valves. These valves release blood into the pulmonary and systemic circulation systems and prevent backflow of blood. Third (S3) and fourth (S4) heart sounds are rare heart sound which are not normally audible but may be visible on the graphic recording. S3 is caused due to rushing of blood from atria to ventricles. S4 is produced when blood is forced into stiff or enlarged ventricle. S1 and S2 are called Fundamental Heart Sounds (FHS).

The period from beginning of one heart beat to the next one is known as the cardiac cycle. In other words, the interval between start of S1 to start of next S1 is called cardiac cycle. The region between S1 and starting of S2 of same heart cycle is called systole and the region between S2 and starting of S1 of next heart sound cycle is called diastole.

Sometimes we may hear unusual sound during the heartbeat cycle. They may be whooshing or swishing noise. These are called murmurs. They are generally high-frequency, noise like sounds that are produced as a result of turbulent blood flow [4]. Different features of PCG signals like intensity, frequency content, split information, time relations, location of murmurs etc. are helpful in detecting heart valve diseases, if any and the state of the heart function. Diastolic murmurs occur after S2, and they are therefore associated with ventricular relaxation and filling. They may be caused by aortic or pulmonic valve regurgitation or by mitral or tricuspid valve stenosis. Systolic murmurs occur between S1 and S2, and therefore they are associated with mechanical systolic and ventricular ejection or regurgitation across the atrio-ventricular valves [4].

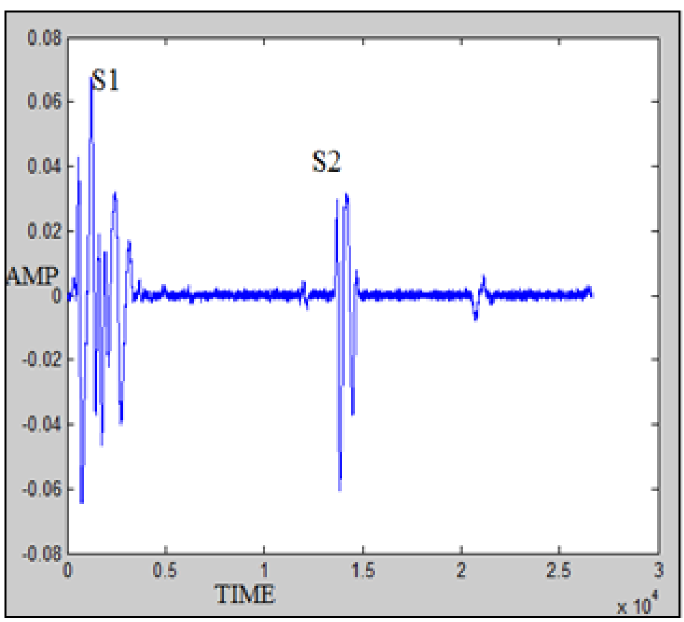

Figure 1.2: A normal PCG signal showing S1 and S2 heart components.

1.3 Aim of Work

Cardiac auscultation is the basic analysis tool for analyzing heart sounds. With the help of auscultation the condition of heart can be examined. Before the symptoms of any heart diseases start showing up, the abnormalities in the heart sounds start appearing. By listening to the heart sounds or with the help of PCG any prevalent heart diseases can be detected at an earlier stage. With the help of PCG the heart sounds can be analyzed in a better way as it also displays the sounds which are sometimes not heard with the help of stethoscope. Further, at later stage more advanced techniques like ECG and echocardiography can be used to study the problem and required precautions can be taken and worsening of the situation can be avoided.

The aim of this study is to classify the heart signals into three classes namely normal signal, systolic murmur signal and diastolic murmur signal. Figures 1.3, 1.4 and 1.5 shows the normal signal, systolic murmur signal and diastolic murmur signal respectively. Causes of systolic murmurs include aortic stenosis (AS), pulmonic stenosis (PS), atrial septal defect (ASD), mitral regurgitation (MR) etc. and causes of diastolic murmurs include mitral stenosis (MS), tricuspid stenosis (TS), aortic regurgitation (AR), pulmonic regurgitation (PR) etc [5]. This classification can help us to diagnose the disease easily and more accurately. Different conditions of heart result in different kinds of murmurs i.e. systolic murmur or diastolic murmur. The classification can therefore help us to understand the state of the heart in a better way. Many features in time, frequency and statistical domains have been extracted from PCG signal. Also, features have been extracted even from systolic and diastolic regions so that systolic and diastolic murmurs can be classified more accurately. A total of 144 signals have been studied in this thesis. The classification of these signals has been done to accurately separate normal, systolic murmur and diastolic murmur signals from each other. Various classifiers have been used for the classification. Also, classification adaptive weighted fischer discriminant ratio algorithm has been developed. Comparison of the classification accuracies using different classifiers has also been done to see which classifier gives us better results for the classification.

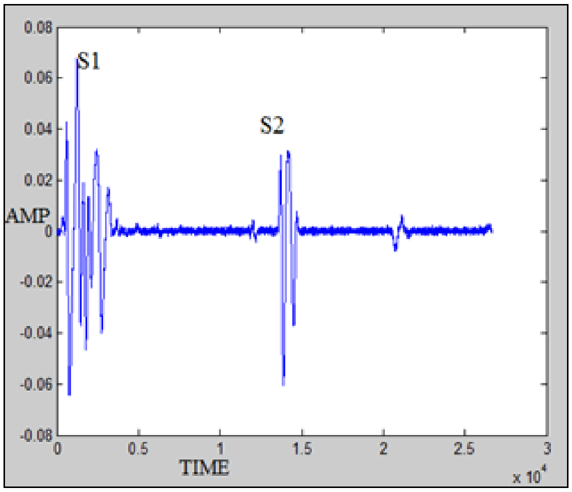

Figure 1.3: A normal PCG signal showing fundamental heart components (FHS).

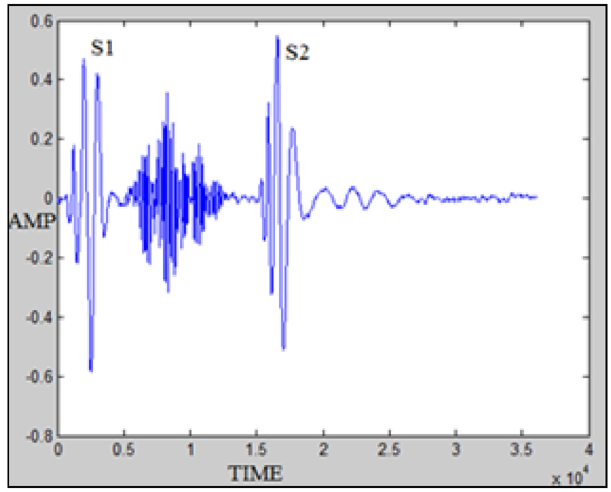

Figure 1.4: PCG signal with systolic murmur.

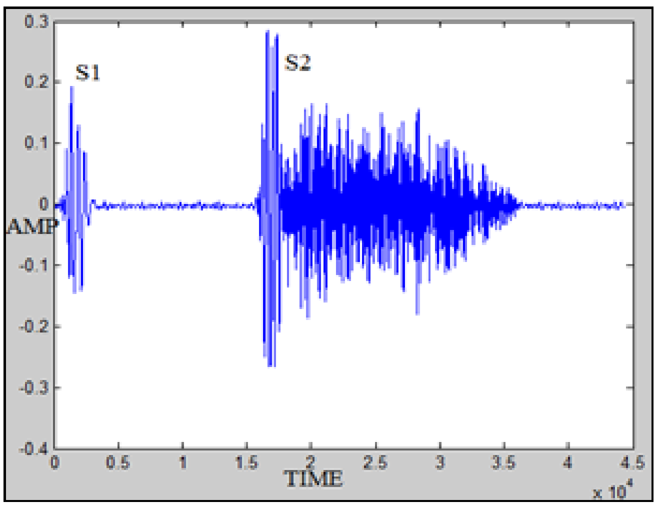

Figure 1.5: PCG signal with diastolic murmur.

1.4 Outline of Thesis

This thesis consists of 6 chapters which have been introduced as follows to get an overview of the study carried out.

Chapter 1 is Introduction. In this chapter the concept of auscultation has been discussed. The advantages of this earlier technique over the new techniques like ECG have been mentioned and discussed. Then the concept of phonocardiography have been introduced and discussed in detail. Our study is based on the phonocardiography as the PCG signals form the basis of our study. After discussing phonocardiography, aim of this study has been explained so as to get a better view of the problem. Then the outline of the thesis is given so as to get an overview of this study.

Chapter 2 is The Heart. In this chapter the importance, structure and working of heart has been discussed. The various types of murmurs and heart defects have been discussed.

Chapter 3 is Literature review. In this chapter the researches that have been done by various researchers have been discussed. The contributions that have been made by various researchers in their studies on PCG signal have been mentioned. Comparisons have also been made for the different methodologies used in various studies. In the end, the previous works discussed have also been summarized.

Chapter 4 is Materials and Methodology. In this chapter various softwares and tools which have been used are mentioned. This chapter also explains the methodology used to carry out this study. The PCG signals which have been used for this study were taken from publicly available dataset and heart sound CD. Then various time, frequency and statistical domain features were extracted. These features were then reduced to get a few features so as to remove the data redundancy and computational load. The best features were selected on the basis of Fisher Discriminant Ratio (FDR) for classification. Various classifiers were used for classification of the signals into pre-defined classes. Also, adaptive weighted FDR algorithm was developed in MATLAB for classification. Also, the features that were extracted were evaluated by plotting each and every feature against another feature to see which features are capable of separating out the three classes. A total of 378 plots were plotted.

Chapter 5 is Results. This chapter includes various feature values which were extracted in order to classify the signals. Also, this chapter includes the various accuracies obtained during the classification of the signals by various classifiers. Confusion matrix has also been plotted.

Chapter 6 is Conclusion and Future scope. In this chapter the conclusion of this study has been mentioned. The significance of the study has been mentioned and the improvements that can be made have also been discussed.

CHAPTER 2

THE HEART

2.1 Importance of Heart

The heart is one of the most vital organs in the entire human body. We can say that it is a pump composed of muscles. It pumps the blood throughout the whole body and beats at a rate of about 72 beats per minute. As the heart pumps blood, it circulates all the vital nutrients which help our body to function properly. It carries oxygen, glucose, amino acids etc. to muscles and all the organs of our body. Also, it carries waste materials from cells and tissues. The carbon dioxide is collected from cells and the deoxygenated blood is circulated to the lungs for purification. The oxygenated blood is circulated to each and every cell of the body [6].

2.2 Anatomy of the Heart

2.2.1 Pericardium

The heart is located within a fluid-filled cavity which is known as the pericardial cavity whose walls and lining are made up of a special which is called as the pericardium. Pericardium helps in lubricating the heart and preventing friction between the heart beating and the organs surrounding the heart as it is a type of serous membrane which produces serous fluid. The pericardium is also responsible for maintaining hollow space so that the heart can expand when filled with blood and to hold the heart in position. The heart wall is made of 3 layers: epicardium, myocardium and endocardium [7].

- Epicardium: It is the outermost layer of the heart wall and is a thin layer of serous membrane. This layer helps in lubrication of the heart and also protects the outside of the heart.
- Myocardium: It is the middle layer of the heart wall that contains the cardiac muscle tissue. It is a muscular layer which makes up the majority of the mass and thickness of the heart wall. It is a part of heart which helps in pumping the blood.

- Endocardium: This layer is the inside lining of the heart. It is a very smooth layer and keeps the blood from sticking to the inside of the heart. It is important as it avoids the formation of deadly blood clots.

2.2.2 Chambers of the Heart

The heart contains 4 chambers out of which two are atria and two are ventricles:

- Right Atrium (RA)
- Left Atrium (LA)
- Right Ventricle (RV)
- Left Ventricle (LV)

The atria are smaller than the ventricles and have thinner, less muscular walls than the ventricles. The upper chambers are called atria and the two atria i.e. the right atrium (RA) and left atrium (LA) are separated from each other by an intra-atrial lining known as septum. The lower chambers are known as ventricles i.e. the right ventricle (RV) and left ventricle (LV) and are separated from each other by an intra-ventricular layer known as septum. Atria are thin walled chambers as compared to the ventricles as atria have to transfer blood from atria to ventricles but ventricles pump blood throughout the body. The right side of the heart consists of deoxygenated blood and the left side of the heart consists of oxygenated blood. The walls of the left ventricle are approximately three times thicker than the right ventricle so that it can withstand high pressures during contractions for pumping blood to the rest of the body whereas the right ventricle has to pump blood to lungs only. The atria act as receiving chambers for blood whereas the ventricles send blood out of the heart and hence are larger and stronger pumping chambers. The ventricles are connected to the arteries that carry blood away from the heart whereas the atria are connected to veins that carry blood toward the heart [7]. Figure 2.1 shows the different chambers and valves of the heart.

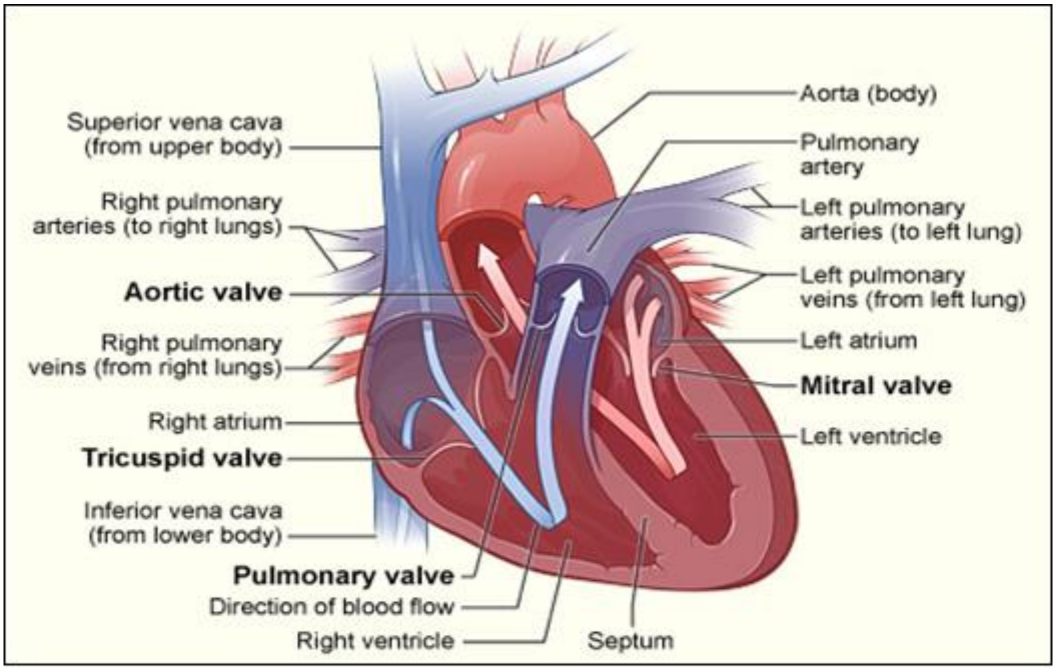

Figure 2.1: The Human Heart [5]

The chambers on the right side of the heart are comparatively smaller and have less myocardium in their heart wall than the left side of the heart. This difference in size between the left and right sides of the heart is due to their functions and also due to the difference in size of the two circulatory loops. The right side of the heart pumps blood to the lungs which are located nearby i.e. it is responsible for pulmonary circulation whereas the left side of the heart pumps blood to the whole of the body i.e. to all the organs of the body i.e. it is responsible for the systemic circulation.

2.2.3 Valves of the Heart

The heart pumps the oxygenated blood to all the organs and tissues of the body and deoxygenated blood to lungs for purification. First of all the blood from atria is pumped to ventricles and then to the lungs and other systems of the body. One-way valves are present so that backflow of the blood into the heart can be prevented. It consists of four valves out of which two are atrioventricular valves and two are semilunar valves. These *four valves* are as follows:

- Mitral or bicuspid valve

- Tricuspid valve
- Aortic Valve
- Pulmonary valve

Figure 2.1 shows all the valves of the heart. The left atrium is joined to the left ventricle through the mitral valve, which is sometimes called as the bicuspid valve since it consists of two cusps. Similarly, the right atrium is joined to the right ventricle through tricuspid valve [3]. The atrioventricular valves prevent the flow of blood back to atria from the ventricles. Between the left ventricle and aorta, the aortic valve is present which is responsible for unidirectional flow of blood i.e. from the left ventricle to aorta. Through aorta the oxygenated blood is supplied to all the systems of the body. In the same way, between the right ventricle and pulmonary artery, pulmonary valve is present. This valves results in one-way flow of blood from right ventricle to pulmonary artery and prevents the backflow of the blood. The pulmonary artery carries deoxygenated blood to lungs for purification i.e. deoxygenated blood is oxygenated by gaseous exchange in the lungs [7].

2.2.4 Conduction System of Heart

The heart itself sets its own rhythm and also conducts the signals which are necessary to maintain and coordinate this rhythm between the atria and ventricles. About 1% of the cardiac muscle cells in the heart form the conduction system. For the rest of the cardiac muscle cells, it sets the pace at which they should contact and relax.

The sinoatrial node (SA) is the natural pacemaker of the heart. The SA node is a small bundle of cells and is located in the wall of the right atrium inferior to the superior vena cava. Its function is to control the heart rate by generating electrical impulses. Figure 2.2 shows the electrical signals coming from SA node. The electrical stimulus from the SA node then reaches the atrioventricular node (AV) which is then delayed for a brief time so that the atria which are contracting pumps all the blood the ventricles. When all the blood from atria gets transferred to ventricles, the valves between the atria and ventricles close. At this point the atria begin to refill and the electrical stimulus passes through the AV node and Bundle of His into the Bundle branches and Purkinje fibers [8].

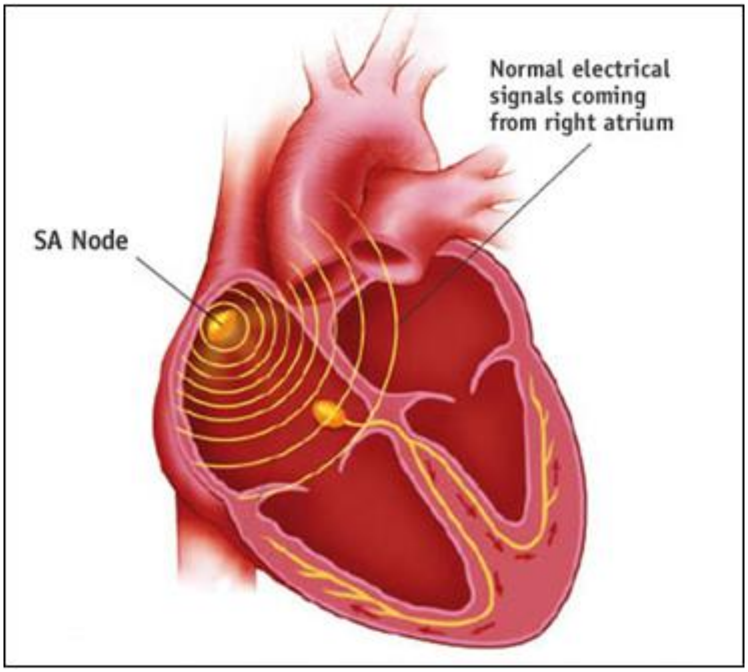

Figure 2.2: Electrical signals coming from Sinoatrial node (SA) [9]

Purkinje fibers carry the signals to the walls of the ventricles which stimulate the cardiac muscle cells to contract in a coordinated manner to efficiently pump blood out of the heart [7].

2.3 Physiology of the Heart

2.3.1 Normal Physiology

Coronary Systole and Diastole

At any given time the chambers of the heart may found in one of two states:

- Systole: The cardiac muscle tissues contract so as to push blood out of the chamber during systole.
- Diastole: The cardiac muscle cells relax so that the blood fills the chambers of the heart. This happens during diastole.

During ventricular systole, blood pressure increases in the major arteries and decreases during ventricular diastole [7].

The Cardiac Cycle

The period from beginning of one heart beat to the next one is known as the cardiac cycle. There are three phases to the cardiac cycle: atrial systole, ventricular systole, and relaxation.

- Atrial systole: The atria contract and push blood into the ventricles during atrial systole. The AV valves remain open but the semilunar valves stay closed so that the blood doesn't re-enter the heart. The atria are much smaller in size as compared to the ventricles, so they only fill about 25% of the ventricles during this phase i.e. atrial systole. The ventricles remain in diastole during this phase.
- Ventricular systole: The ventricles contract and push the blood into the aorta and pulmonary trunk during the ventricular systole. The pressure created in the ventricles forces the semilunar valves to open but the AV valves remain closed. Due to this the blood flows from the ventricles into the arteries and backflow of blood doesn't occur. After this, the cardiac muscles of the atria repolarize and enter the state of diastole during this phase.
- Relaxation phase: All 4 chambers of the heart are in diastole as blood flows into the heart from the veins during the relaxation phase. The ventricles are filled to about 75% capacity during this phase. Only after the atria enter systole, the ventricles are completely filled. During this phase, the cardiac muscle cells of the ventricles are repolarized so as to prepare for the next round of depolarization and contraction. Also, the AV valves open up so as to allow the blood to flow freely into the ventricles but the semilunar valves close to prevent the regurgitation of blood from the great arteries into the ventricles [7].

Deoxygenated blood which returns from the body first enters the heart from the superior and inferior vena cava. Then the blood enters the right atrium which is then pumped through the tricuspid valve into the right ventricle. From the right ventricle, the blood is pumped into the pulmonary artery through the pulmonary semilunar valve.

The pulmonary artery carries blood to the lungs where it releases carbon dioxide and absorbs oxygen i.e. gases are exchanged. The blood in the lungs returns to the heart through the pulmonary veins. From the pulmonary veins, blood enters the left atrium of the heart again.

Then the left atrium contracts to pump blood through the bicuspid (mitral) valve into the left ventricle. The left ventricle then pumps blood through the aortic semilunar valve into the aorta. From the aorta, blood enters into systemic circulation throughout the body tissues until it returns to the heart via the vena cava and the cycle repeats. Figure 2.3 shows the events which take place during one cardiac cycle.

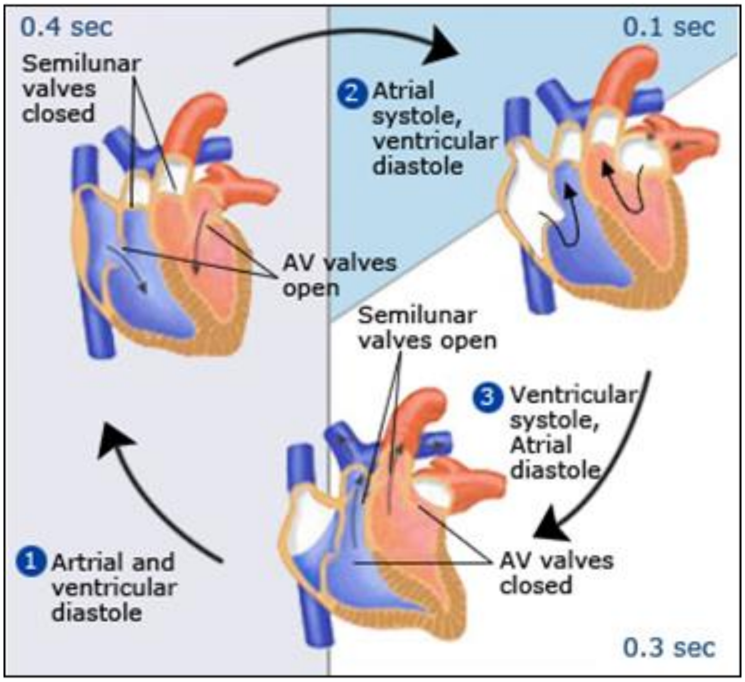

Figure 2.3: Cardiac Cycle of the Heart [10]

2.3.2 Abnormal Physiology

The functioning of the heart can be disrupted because of many reasons. The problem could be genetic or it may have been developed with time. Deoxygenated blood from the body enters the right atrium which is then passed into the right ventricle and is finally ejected into the pulmonary artery on the way to the lungs. Oxygenated blood from the lungs then re-enters the left atrium of the heart. It then passes into the left ventricle which is pumped to the whole body through the aorta. The genetic problem could be that the septum or muscular partitioning between the two halves of the ventricles could have a hole. So, the mixing of blood in the left (oxygenated) and right (deoxygenated) ventricles take place and hence cause improper functioning of the heart.

This is called septal defect. Due to this the person feels fatigued as proper oxygen is not received by the cells and tissues of the body.

The non-genetic problem could be due to calcination of valves or due to cholesterol deposition which causes thickening of the valves. This impedes the normal blood flow and is a major cause of acquired heart diseases. Another reason of a heart disease can be a leaking valve. Sometimes, the valves don't close properly and blood leaks back into the atrium. This impedes the normal functioning of heart.

2.4 Heart Sounds

2.4.1 Normal Heart Sounds

The blood flow is normally laminar in nature but when the blood passes through a small opening or has some obstruction in its path then the flow becomes turbulent. This is the reason behind the fact that when blood passes through the valves which have small openings, the blood flow becomes turbulent. Due to this turbulence along with the vibrations caused by closure of heart valves results in the vibrations of the heart and the blood as an interdependent system. These vibrations according to cardiohemic theory are believed to be the basis of heart sounds. The normal heart sounds are:

S1: The heart sound that occurs with ventricular systole and is produced mainly by closure of the atrio-ventricular valves.

S2: The heart sound that signifies the beginning of diastole and is caused by closure of the semi lunar valves.

S3: The heart sound that occurs in early diastole and corresponds with the first phase of rapid ventricular filling.

S4: The heart sound occurring in late diastole, corresponding with atrial contraction [11].

The region between S1 and S2 is termed as systole. The region between S2 and next cycle's S1 is termed as diastole. Systole is smaller than diastole.

Out of these four heart sound components, the dominant two are S1 and S2 which are commonly known as Fundamental Heart Sounds (FHS). These two sounds are mainly audible sounds and other two are usually not audible. These two sounds are called 'lub' and 'dub' in common terminology (refer figure 2.4). In medicine we call the lub sound as 'S1' and the dub sound as 'S2'. The normal heart rates at rest are 60 to 100 beats or lub-dubs per minute.

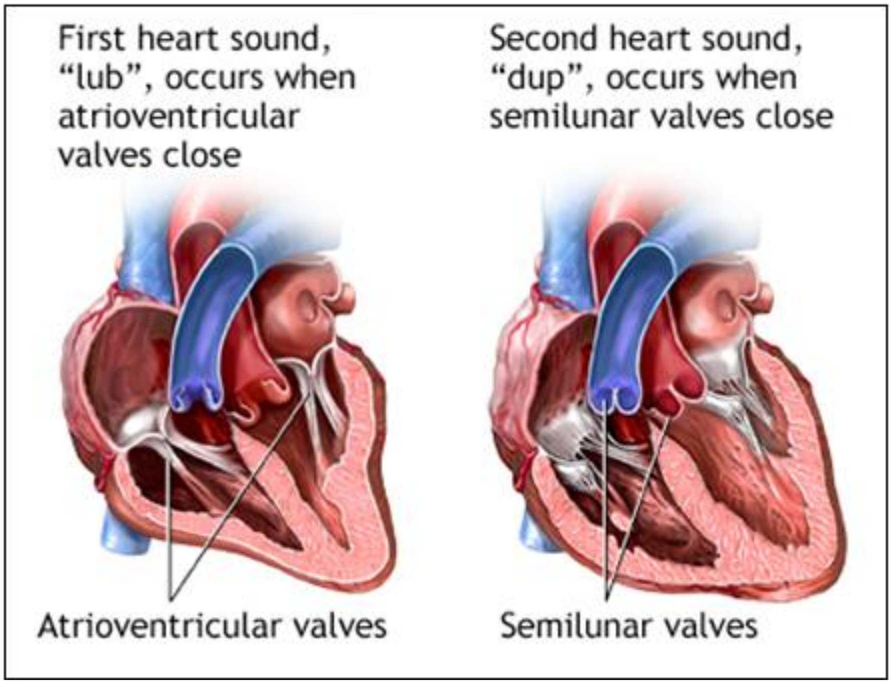

Figure 2.4: Production of Fundamental Heart Sounds [12]

2.4.2 Abnormal Heart Sounds

Sometimes other than the normal heart sounds some extra sounds are also heard. These extra sounds may be evident because of some heart problems which may be present or developing. Some abnormal heart sounds are as follows:

Murmurs

These are long strings of noise that can't be termed as a single sound is termed as Murmurs. Murmurs are caused by the blood turbulence and can be heard using a stethoscope. They may be whooshing or swishing noise. They are generally high-frequency, noise like sounds. The murmurs can be termed as the indicators to various heart problems. Also if some extra blood turbulence is created it may be conclude that the blood is flowing through a few extra small openings, other than just passing through the valves. As shown in figure 2.5, these are mainly of two types depending upon their location of occurrence.

- Systolic murmur: The murmur which appears in the region between S1 and S2 (known as systole) is termed as systolic murmur.
- Diastolic murmur: The murmur which appears in the region between S2 and next cycle's S1 (known as diastole) is termed as diastolic murmur.

Sometimes, the murmurs occur throughout the cardiac cycle. Then they are termed as continuous murmurs.

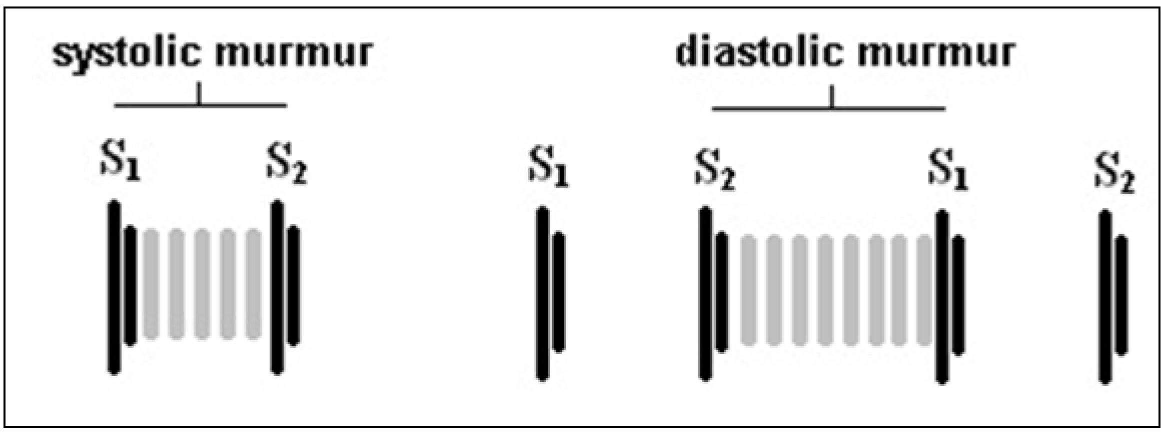

Figure 2.5: Systolic and Diastolic murmurs [13]

Various causes of murmurs

The problem causing murmurs could be congenital or may have been developed with time. The congenital problem is that which is present right from the birth itself. One of the reasons could be that the septum or muscular partitioning of the ventricles or atria may have a hole. So, mixing of blood from left (oxygenated) and right (deoxygenated) ventricles take place and hence cause improper functioning of the heart and efficiency of the person is reduced. This is called septal defect. This leaking of blood from small hole present on the septum causes blood turbulence and hence the murmurs [14]. Figure 2.6 shows normal heart and heart with ventricular septal defect due to which blood in left and right ventricles gets mixed up and reduces the efficiency of the person.

The acquired heart problem could be due to calcination of valves or due to cholesterol deposition and hence causes thickening of the valves. This impedes the normal blood flow and is a major cause of acquired heart diseases. Another reason of a heart disease can be a leaking valve. Sometimes the valves don't close properly and blood leaks back into the atrium. This impedes the normal functioning of heart. These reasons can also cause blood turbulences and hence the murmurs [14].

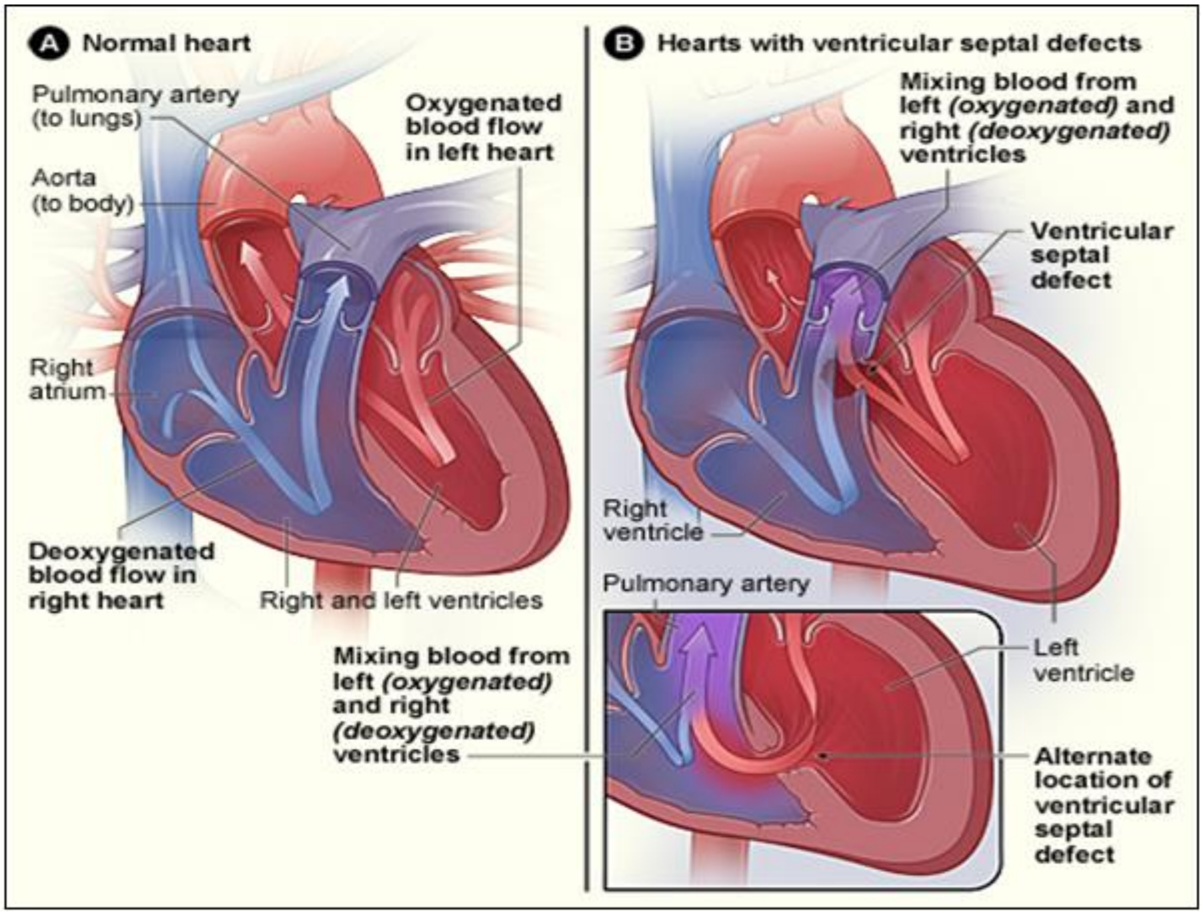

Figure 2.6: One of the causes of murmurs i.e. Ventricular Septal Defect (VSD) [14]

Clicks

Clicks are the extremely short duration sounds and hence their name. As shown in figure 2.7, they appear during systole. These can be easily differentiated from the murmurs which are longer in duration and can appear both in systole and diastole.

Types of clicks

- Early systolic: Just after S1 high pitched click is heard in association with the "opening snap" of the semilunar valves which are mildly to moderately stenotic.
- Mid-systolic click: A medium pitched variable sound is commonly heard in association with mitral valve prolapse.

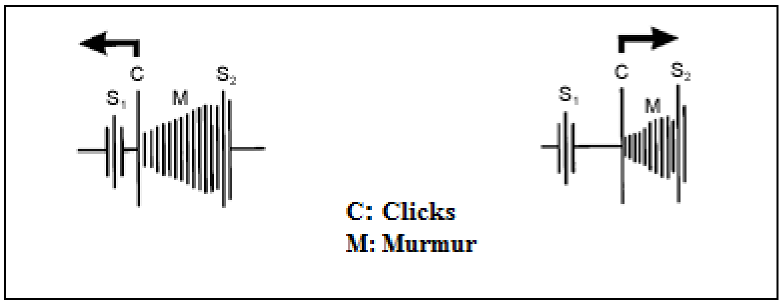

Figure 2.7: Clicks and murmurs in a heart signal [15]

CHAPTER 3

LITERATURE REVIEW

Heart sounds provide valuable information about the health of the heart. Therefore, since the invention of stethoscope auscultation is used for diagnosis of heart valve disorders. It is a primary detection tool. Many researchers have studied PCG signals using various signal processing techniques. Firstly, pre-processing of heart signals is done. Pre-processing include normalization, segmentation, noise removal etc. After pre-processing features are extracted and then the extracted features are used for classification. Most of the studies use wavelet transform for studying PCG signal [16-23]. Some researchers have used spectral analysis, decision trees and time-frequency analysis, FFT [24-26]. In many studies segmentation of heart sounds into cardiac cycles have also been done before feature extraction phase using ECG gating [16, 17].

Many researchers have done various studies in this field and contributed in different ways in studying and classifying heart signals. Following are some of the related work done by various authors.

Z. Sharif *et al* (2000) classified heart sounds and murmurs for heart diseases with the use of instantaneous energy and the frequency estimation. A set of 102 heart sound signals were used for the analysis. To estimate the instantaneous energy and frequency the central finite difference frequency estimation (CFDFE) and zero crossing frequency estimation (ZCFE) techniques were used. Both these methods use the same techniques to estimate instantaneous energy but to estimate instantaneous frequency difference is there. Features of heart sound signals were defined by estimating the instantaneous energy and frequency which can be further used so that the various heart sounds can be uniquely discriminated or classified [27].

R. Amarnath *et al* (2003) compared various methods of classification of heart diseases. For classification various time domain, frequency domain and statistical features were calculated. He used neural network fuzzy system and wavelets and accuracy of each method was compared. The classification accuracy of 92% was achieved using wavelet method, 85% using neural networks and 88% using fuzzy system. They concluded that the wavelet method classifies the heart sounds more accurately into normal and abnormal as compared to other classifiers used [28].

M. El-Seiger *et al* (2005) used STFT for detection of first and second heart sounds (S1 & S2). Also, for murmur analysis he used 20-70% of the systolic segment as heart signals S1 and S2 sometimes partially overlap systolic murmur [29].

Z. Jiang *et al* (2006) proposed analytical model which was based on single DOF. Characteristic waveforms were extracted using this model from heart sounds to detect heart disorders. The diagnostic parameters [T1, T2, T11, T12] were obtained by FCM clustering method. For cardiac sound characteristic waveform (CSCW) scattergram and histogram were plotted for [T1, T2] and [T11, T12] [2].

A.L. Noponen *et al* (2007) differentiated innocent murmurs and pathological murmurs using phono-spectrographic analysis. The study showed that innocent murmurs are characterized by lower frequency and have a frequency spectrum with more harmonic structure as compared to pathological cases [30].

V. Nigam *et al* (2008) proposed a method to locate systolic murmurs in the PCG signal based on their visual simplicity which is independent of their absolute amplitude and frequency characteristics. Fuzzy clustering approach was used and it showed that number of fuzzy clusters can be used to determine presence of cardiac murmurs. The degree of membership of simplicity value in clusters was used to locate systolic murmurs. The accuracy achieved in detecting systolic murmurs was 80% [31].

E. Delgado-Trejos *et al* (2008) analyzed three families of features: (a) time-varying & time-frequency features (b) perceptual and (c) fractal features. They found out that the fractal features applied to the detection of murmurs emerged as the most robust characteristics in the sense of accuracy vs. computational load [32].

J. Vepa (2009) derived features from cepstrum of the heart sound signals and were compared with features extracted from short-term Fourier transform (STFT) and discrete wavelet transform (DWT) [33].

I. Maglogiannis *et al* (2009) proposed an automatic diagnostic system which was based on Support Vector Machine (SVM) to identify various heart valve diseases. Four heart valve diseases were taken into account: aortic stenosis (AS), aortic regurgitation (AR), mitral stenosis (MS) and mitral regurgitation (MR). The heart sounds were first classified into normal and disease-related. The disease related heart sounds were further classified into heart sounds with systolic or diastolic murmurs. The heart sounds with systolic murmur were classified using SVM into heart sounds having aortic stenosis or mitral regurgitation and those with diastolic murmurs were classified using SVM into heart sounds having aortic regurgitation or mitral stenosis. Accuracy of 91.4% was achieved in classifying normal and abnormal heart sounds. In classifying systolic and diastolic murmur signals accuracy of 91.25% was achieved. In third stage classification, in classifying aortic stenosis or mitral regurgitation the accuracy of 91.67% was achieved, while for the classification as aortic regurgitation or mitral stenosis the accuracy of 93.42% was achieved [34].

S. Ari *et al* (2010) classified normal and abnormal heart sounds and the classifier used was least square support vector machine (LSSVM) classifier using wavelet based feature set. Results showed that the proposed technique had greater accuracy than standard SVM and classical least square SVM [35].

S. Choi *et al* (2010) proposed a novel cardiac sound spectral analysis method using the normalized autoregressive power spectral density (NAR-PSD) curve with the support vector machine (SVM) technique for classifying the cardiac sound murmurs. Also two diagnostic features Fmax and Fwidth were proposed which described the maximum peak of NAR-PSD curve and the frequency width between the crossed points of NAR-PSD curve on a selected threshold value. The results showed the diagnostic parameters for normal cases were concentrated at low frequency region and had small width due to low-density of frequency, while the values in the abnormal cases were distributed on the high frequency region and scattered widely in comparison with the normal cases [36].

L.H. Cherif *et al* (2010) highlighted the importance of the choice of wavelet. He analyzed the PCG signal using discrete wavelet transform (DWT) and packet wavelet transform (PWT). It was seen that in case of filtering clicks and murmurs DWT is more suited than wavelet packet transform. If one wants to do filtering of the murmurs such that there is not much distortion of S1 and S2 heart sound components, DWT is likely to be used whereas when PWT is applied morphology of internal components are affected much more as compared to when DWT is applied. Various wavelets and their order were used for the analysis and it was concluded that by analyzing wavelet db7 distinction between sounds and various heart can be done easily using DWT or PWT. Qualitative study of systolic and diastolic murmurs and clicks of PCG signals can be carried out more efficiently using DWT but PWT provide better information which gives better comprehension of time-frequency characteristics of heart sounds, internal components, heart murmurs and clicks [37].

S. Yuenyoung *et al* (2011) proposed an algorithm in which cardiac cycles were extracted from heart sounds with different heart rates. Using this algorithm there was no need to label the individual Fundamental Heart Sounds (FHS) for extraction of individual heart cycles. Discrete wavelet transform was used for feature extraction of cardiac sounds and classification was done using neural network bragging predictors [38].

S. Sanei *et al* (2011) used Adaptive Singular Spectrum Analysis (ASSA) to separate murmurs from the recorded heart sounds. The major advantage of this technique is in perfectly separating the two sounds even in temporally overlapped regions [39].

M.A. Akbari *et al* (2011) proposed a new analytical technique which he named as Digital Subtraction Phonocardiography (DSP). This technique is based on the principle that the murmurs are random in nature but the Fundamental Heart Sounds (FHS) are deterministic in nature. The difference between the acoustic emissions of two successive heart beats was simply taken and murmurgram was constructed. It was found that for normal cases the murmurgram should be flat between the FHS but for abnormal cases i.e. heart sounds with murmurs this wasn't the case [40, 41].

R.R. Sarbandi *et al* (2011) proposed a new technique known as Color Spectrographic Phonocardiography (CSP). It was used to detect and characterize heart murmurs [42].

H. Xiao-Juan *et al* (2011) extracted S3, S4, the first split and the second split and relocated the starting and ending of S1 and S2. It was based on the slopes of envelop of Hilbert Transfer Envelope after energy segmentation. In this research the overall accuracy of 91.95% was achieved for features extraction. 25 significant clinical features were introduced and SVM classifier was used for classification. The overall accuracy of 91.3% was achieved in case of classification. The result showed that features including clinical signification is of signification for enhancing the accurate rate of Phonocardiogram classification [43].

S. M. Debbal *et al* (2012) used Continuous Wavelet Transform (CWT). He studied normal and abnormal Phonocardiogram signals. He extracted features in time-frequency domain and their scalograms were plotted. It was seen that they exhibited noticeable morphological differences in terms of duration and spectral composition of sounds [44].

F. Safara *et al* (2012) introduced new entropy to analyze heart sounds and it was shown that it was feasible to use this entropy in classification of five types of heart sounds and murmurs. The heart sounds considered for classification consisted of one normal heart sound and four common murmurs: Aortic regurgitation, Mitral regurgitation, Aortic stenosis, and Mitral stenosis. Heart sound analysis was done by wavelet packet transform. To derive various feature vectors the entropy was calculated. Five types of classification were performed and the accuracy of the generated features was evaluated. The best results were achieved using Bayes Net as a classifier with an accuracy of 96.94%. The results showed that the proposed wavelet packet entropy was effective for heart sounds classification [45].

H. Uguz (2012) developed biomedical based decision support system to classify heart sound signals. The heart sound signals were obtained from 120 subjects and comprised of normal, pulmonary and mitral stenosis heart valve diseases. These signals were obtained via stethoscope. The developed system comprised of 3 stages: feature extraction, feature reduction, and classification. In feature extraction stage, discrete wavelet transform (DWT) was applied to separate heart sound signals to its sub-bands. In second stage, the dimensionality of feature vectors was reduced using Shannon energy algorithm. Entropy of each sub-band was calculated. In the third stage, the features which were reduced earlier in second stage were given as input to adaptive neuro-fuzzy inference system (ANFIS) classifier to classify it into the 3 mentioned categories. Maximum classification accuracy of 98.33% was achieved [46].

Y. Chen *et al.* (2012) used continuous wavelet transform instead of the discrete wavelet transform on the heart sound data for distinguishing innocent murmurs from organic murmurs. A matrix was derived from the continuous wavelet transform which was then processed via singular value decomposition and QR decomposition for feature extraction [47].

H. Sun *et al* (2013) combined Improved EMD (Empirical Mode Decomposition) and Shannon energy envelope algorithm for extraction of S1 and S2 components and achieved a high accuracy of 99.74% [48].

F. Safara *et al* (2013) proposed multi-level basis selection (MLBS). This was done by removing the less informative bases and was done so that the most informative bases of the wavelet packet transform decomposition tree is preserved. Three exclusion criteria i.e. frequency range, noise frequency, and energy threshold was applied. The classification was done between normal heart sound signal and three kinds of murmur signals (mitral regurgitation, aortic regurgitation and aortic stenosis). It was found out that an accuracy of 97.56% was achieved using MLBS. Also, the results were compared with single-level basis selection (SLBS), local discriminant basis (LDB) and best basis selection (BBS) and it was found out that higher accuracy was achieved with MLBS [49].

M. Singh and A. Cheema (2013) proposed a new feature, mean12, which is the maximum of the mean in systolic and diastolic region to classify signal into two classes i.e. normal and murmur signal. 23 features in time domain, frequency domain, statistical and cepstrum were extracted and out of all the features only 5 optimal features were selected for classification. Four different classifiers were used and the accuracies were calculated. Also, 5 fold cross validation was used. The classifiers used were Bayes Net, Naïve Bayes, SGD and Logit boost and the accuracies achieved were 91.6%, 93.3%, 91.6% and 88.3% respectively. Highest accuracy of 93.3%was achieved using the Naïve Bayes classifier [50].

S. Patinder S. and R.M. Pachori (2014) proposed a new method for classification of heart sound signals. The features which were extracted from the heart beat cycles which were reconstructed separately from the heart sounds and murmurs. They used constrained tunable Q-wavelet transform (TQWT) to separate heart sounds and murmurs. The features that were extracted were based on time-domain, TQWT and (Fourier- Bessel) FB expansion. The features were selected to reduce the obtained feature set and classification was done using least square SVM (LS-SVM) with various kernel functions. The performance of this method was even validated with publically available datasets. The results were compared with STFT based method when applied on the available dataset. The overall classification accuracy of 94.01% was achieved using the proposed method with RBF kernel against 93.53% in case of STFT based method [51].

Table 3.1: Comparison table of different methodologies used in various studies

Year	Methodology	Contributions	Performance achieved	ECG gating used	Comments
2005	Short Time Fourier Transform (STFT) [29]	Detection of heart sounds (S1 & S2) and systolic murmur.	100%- S1 97%- S2	Yes	20-70% of systolic segment was selected for murmur detection analysis.
2006	Cardiac Sound Characteristic Waveform (CSCW) [2]	Arrhythmia, Mitral Stenosis, Aortic Regurgitation		No	Adaptive Threshold Value was calculated using Fuzzy C-Means.
2007	Phonospectrogram [30]	Characterization of innocent murmurs in children	90%- Sensitivity 91%- Specificity	No	Innocent murmurs have lower frequencies and frequency spectrum with more harmonic structure as compared to pathological murmurs.
2008	Fuzzy clustering [31]	Location/ detection of systolic murmur	80%- Detection 73%- Sensitivity 100%- Specificity	No	An amplitude and frequency invariant signal characteristic has been proposed to distinguish cardiac murmur.
2011	Discrete Wavelet Transform [38]	High noise robustness	92%- Noise-free 90%- with white noise and 10 dB SNR and for impulse noise up to 0.3s duration.	No	No segmentation used.
2011	Adaptive Singular Spectrum Analysis (ASSA) [39]	Extraction of different types of murmur signal.	Correlation between separated components, heart sound and murmur signal	No	Two sounds are separated perfectly even if they are temporally overlapped over a region.

Year	Methodology	Contributions	Performance achieved	ECG gating used	Comments
2011	Digital Subtraction Phonocardiography [40,41]	Murmurgram	Visual differences	Yes	Normal murmurgram is fairly flat and low in intensity
2011	CSP (Color Spectrographic Phonocardiography) [42]	Distinguish pathological and innocent murmurs in children	Visual differences	Yes	Pathological systolic murmurs have lower frequency and shorter duration than innocent systolic murmurs
2011	Hilbert Transfer Envelope [43]	Classification of normal and abnormal PCG signals	Accuracy-91.3%	No	Energy of each segment (0.01s time) is calculated and energy plot is obtained.
2012	CWT (Continuous Wavelet Transform) [44]	Scalogram	Visual differences	No	Temporal and frequency rates are considered to quantify the differences between various PCG signals.
2012	Wavelet Packet transform [45]	Distinguish normal, mitral stenosis, mitral regurgitation, aortic stenosis, and aortic regurgitation	Accuracy-96.94%	No	Wavelet packet entropy was used to calculate or generate features from PCG recordings which are discriminative in nature.
2013	Improved EMD (Empirical Mode Decomposition) [48]	PCG signal denoising and extraction of 1st and 2nd heart sounds	S1- 100% S2- 99.48% overall accuracy-99.74%	No	Signal is decomposed into several different frequency bands from high frequencies to low frequencies.
2013	Wavelet Packet transform [49]	Distinguish normal heart sound, mitral regurgitation, aortic regurgitation and aortic stenosis.	Accuracy-97.56%	Yes	Multi-level basis selection (MLBS) was proposed so that the most informative bases of a wavelet packet decomposition tree is preserved.
2013	Feature extraction in time domain, frequency domain and statistical features [50]	A new feature, mean12, is proposed which is the maximum of the mean in systolic and diastolic regions.	Bayes Net- 91.6% Naïve Bayes-93.3% SGD- 91.6% Logit boost-88.3%	No	Classification of normal and abnormal heart sounds is done.

Different methodologies have been used by various researchers for studying and classifying heart sound signals. Many features have been extracted by different researchers in different domains. Time, frequency, statistical and cepstral features were extracted in different studies [27, 28, 32, 33]. Wavelet transform (discrete wavelet transform, continuous wavelet transform etc.) has been extensively used as a technique for feature extraction [16-23, 35, 37, 38, 44]. Wavelet packet entropy was introduced by Safara *et al* for analyzing heart sounds [45]. Various clustering methods were used in different studies [2, 31, 51]. SVM classifier was used by many researchers in their studies for classification of heart sounds and it was seen that it achieved decent accuracy in properly classifying the heart sounds into different classes [22-24, 31, 39]. Some of the researchers studied different types of murmurs [31, 32]. Classification of normal and abnormal heart sounds (with murmurs) was done in some of the studies [28, 35, 40, 41, 44, 50]. Also, classification between normal and various different types of murmur was also done by some of the researchers [34, 45, 46, 49].

CHAPTER 4

MATERIALS AND METHODOLOGY

4.1 Materials Used

As we know that heart sound signal gives us valuable information about the heart condition, the PCG signal is capable of diagnosing various heart diseases at an earlier stage. Therefore, signal processing techniques can be employed to process the PCG signals towards improving the accuracy of diagnosis [52]. Various materials which were used in this study are as follows:

- Publically available database was taken for this which is available at www.peterjbentley.com and from audio CD [53, 54]. The sample rate of the signals is 44100 Hz.
- MATLAB version 7.11.0.584 (R2010b) was used to develop algorithm to classify the heart sounds into three classes: NORMAL, SYSTOLIC and DIASTOLIC signals. Also, it was used to calculate values of various features.
- Spectrum Analyzers: Sigview and Spectra Pus SC were used to calculate the values of some features.
- Microsoft Excel 2007 was used to accumulate the values of all the features. It was also used to do pre-processing.
- WavPad Sound editor by NCH Software was used to divide the signals into individual heart cycles.

4.2 Methodology

The methodology used in this study to classify various heart sounds into pre-defined classes consists of 4 stages: Signal Acquisition, Feature Extraction, Feature Reduction, and Classification as shown in figure 4.1.

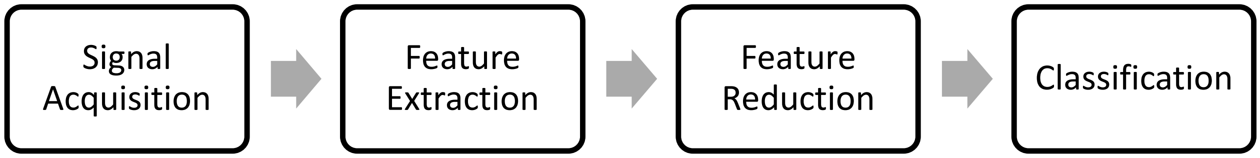

Figure 4.1: Different stages of the methodology used.

4.2.1 Signal Acquisition

PCG signal is a voice signal which is recorded using the electronic stethoscope. The acoustic signals are converted into electronic signals. The recorded signals are then converted to digital signals and plotted to form a phonocardiogram on the computer screen. Sometimes pre-processing is also done on the acquired signal. The signal may be filtered, normalized, scaled or segmented for further analysis.

The database used in this work has been taken from www.peterjbentley.com and from audio CD [53, 54].

4.2.2 Feature Extraction

It is believed that everything in nature is correlated. So, the signals of same class will be correlated with the help of some features. Our motive is to find the features which can correlate the signals of the same class and hence have the potential to discriminate between signals of different classes.

Any parameter which has the potential to discriminate between different classes is termed as a feature. PCG signal is studied carefully and different features are extracted out of a cardiac cycle of the signal. Various features have been extracted to discriminate between the normal, systolic murmur and diastolic murmur signals. A total of 28 features are extracted in this study which are of various domains including time domain, frequency domain and statistical domain. The feature values in even calculated in systole and diastole regions instead of calculating only in the cardiac cycles. This is done as we have to classify signals into systolic murmur and diastolic murmur signals. The extracted feature values are recorded and compiled in Microsoft Excel.

The features that have been extracted in this study are explained below. The suffix 1 and 2 used denote the feature value in systolic region and diastolic region respectively.

- **Total Power**: Total power of the signal is calculated. Normal signals have comparatively lower power.
- **Peak Amplitude**: It is defined as the maximum amplitude of the signal.
- **Peak Frequency**: It is defined as the frequency where maximum amplitude occurs.
- **Mean**: It is the average value of the signal.
- **ZCR**: It is defined as the rate of sign changes that occurs in the signal. In other words, the rate at which sign of the signal changes from positive to negative or vice-versa. Normal signals should have lower value for this feature.
- **ZCR1**: It is the ZCR in systolic region. Value of this feature must be higher for systolic murmur signal as compared to normal and diastolic murmur signals.
- **ZCR2**: It is the ZCR in diastolic region. Value of this feature must be higher for diastolic murmur signal as compared to normal and systolic murmur signals.
- **RMS**: It is defined as the root mean square value of the signal. Normal signals should have lower value for this feature as compared to systolic and diastolic murmur signals.
- **RMS1**: It is the root mean square value of the signal in systolic region. The value of this feature must be higher for systolic murmur signals as compared to other two classes.
- **RMS2**: It is the root mean square value of the signal in systolic region. The value of this feature must be higher for systolic murmur signals as compared to other two classes.
- **Ta**: As shown in figure 4.2, it is time in systolic region starting from S1 till the murmur lasts. It must be greater for systolic murmur signals.
- **Tb**: As shown in figure 4.3, it is time in diastolic region starting from S2 till the murmur lasts. It must be greater for diastolic murmur signals.

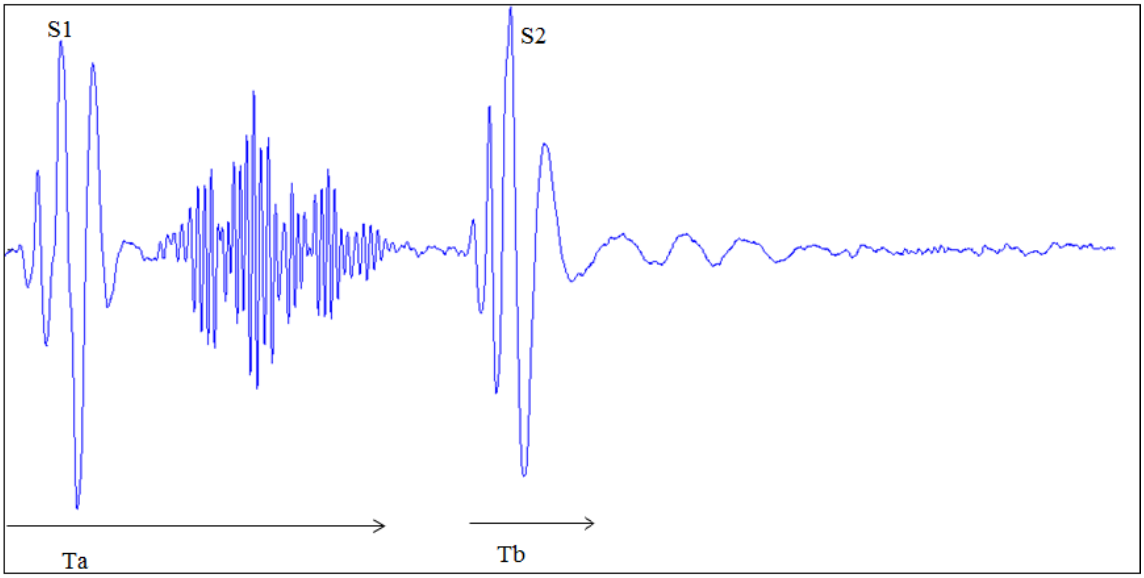

Figure 4.2: Figure showing Ta and Tb in systolic murmur signal.

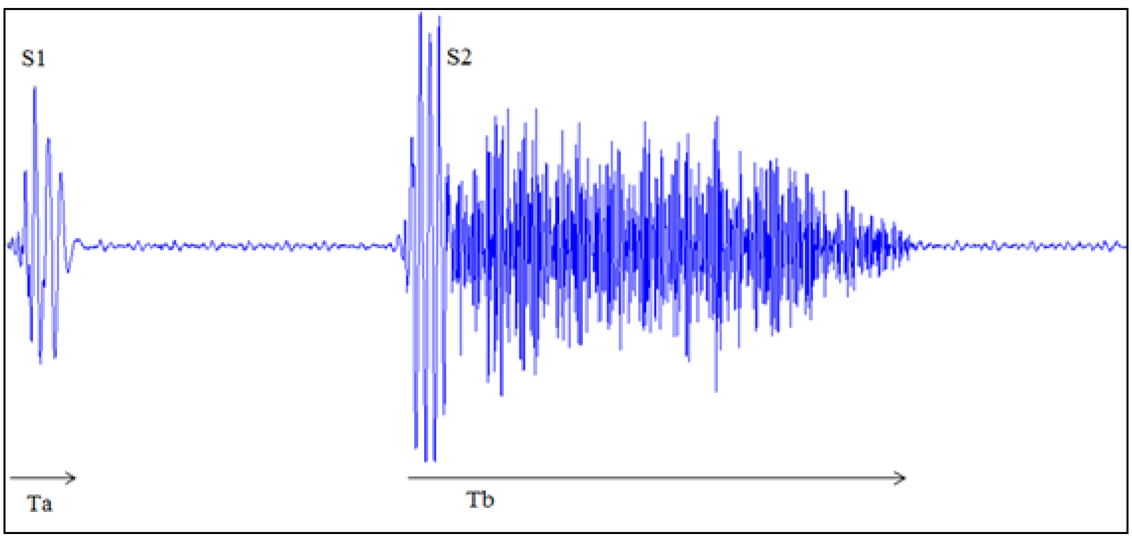

Figure 4.3: Figure showing Ta and Tb in diastolic murmur signal.

- **Max1**: It is the maximum value of the signal in systolic region. The value of this feature is expected to be higher in case of systolic murmur signals as compared to diastolic murmur signals and normal signals.
- **Max2**: It is the maximum value of the signal in diastolic region. The value of this feature is expected to be higher in case of diastolic murmur signals as compared to systolic murmur signals and normal signals.

- **IMD**: It is the amplitude modulation of signals containing two or more different frequencies in a system with nonlinearities.
- **THD**: It is the measurement of the harmonic distortion present in the signal. It is defined as the ratio of sum of all the powers of harmonic components to power of fundamental frequency.
- **Peak frequency(s)**: It is defined as the maximum frequency of the signal. It is the spectral peak frequency.
- **Peak frequency(p)**: It is defined as the maximum frequency of the signal. It is the peak hold peak frequency.
- **BW(s)**: It is defined as the difference between lowest and highest frequency in the signal. This is the spectral BW of the signal.
- **BW(p)**: It is defined as the difference between lowest and highest frequency in the signal. This is the peak hold BW of the signal.
- **Q-factor(s)**: Higher the Q-factor, slower the oscillations die out in the signal. It is the spectral value of the Q-factor.
- **Q-factor(p)**: Higher the Q-factor, slower the oscillations die out in the signal. It is the peak hold value for Q-factor.
- **Crest Factor**: It is defined as the ratio of peak value to RMS value of a waveform. Higher crest factor indicate peaks.
- **Dynamic Range**: It is the ratio of max value to the minimum value in a waveform. Max is the maximum value of the signal.
- **Standard deviation**: It is defined as the amount of variation in the set of data values.
- **Variance**: A small variance indicates that the data points tend to be very close to the mean and hence to each other, while a high variance indicates that the data points are very spread out around the mean and from each other.
- **Skewness**: Skewness is the measure of asymmetry of the data.
- **Kurtosis**: Positive value of kurtosis indicates that the signal is peaked and negative value of kurtosis indicates signal is flat.

Table 4.1: List of features that were extracted for classification.

S. No	Feature	Feature Domain	Feature Source
1	Peak frequency	Frequency	[28]
2	Peak amplitude	Time	[55]
3	Total power	Time	[28]
4	Total Harmonic Distortion (THD)	Frequency	[50]
5	Intermodulation Distortion (IMD)	Frequency	
6	Peak frequency(s) (Spectral)	Frequency	
7	BW(s) (Spectral)	Frequency	[50]
8	Q-factor(s) (Spectral)	Frequency	[50]
9	Peak frequency(p) (Peak hold)	Frequency	
10	BW(p) (Peak hold)	Frequency	[50]
11	Q-factor(p) (Peak hold)	Frequency	[50]
12	Ta (time period from S1 till murmur lasts)	Time	
13	Tb (time period from S2 till murmur lasts)	Time	
14	Crest factor	Frequency	
15	Dynamic range	Frequency	
16	Mean	Statistical	
17	Standard deviation	Statistical	
18	Variance	Statistical	
19	Skewness	Statistical	[28]
20	Kurtosis	Statistical	[28]
21	Zero Crossing Rate (ZCR)	Time	[56]
22	ZCR1	Time	
23	ZCR2	Time	
24	RMS	Time	
25	RMS1	Time	
26	RMS2	Time	
27	Max1 (proposed)	Time	
28	Max2 (proposed)	Time	

4.2.3 Feature Reduction

This is the third stage of the methodology used. In this stage out of the extracted features, a few are selected so that misleading and redundant features are removed. Feature reduction also reduces the dimensionality and computational load. Best features are selected out of all the extracted features which can do classification with higher accuracy. It is one of the important stages so that classification is done properly and with higher accuracy. There are various methods for feature reduction process. Some of them are Principal Component Analysis (PCA), Box plot method, Fisher's Discriminant Ratio (FDR). Here, in this study s FDR method has been used for selection of features for classification. FDR is defined by the following equation:

$$FDR = \frac{|\mu_1 - \mu_2|^2}{\sigma_1^2 + \sigma_2^2} \tag{4.1}$$

In equation (4.1), μ and σ represents the *mean* and *standard deviation* of a feature and the subscripts *1* and *2* represent class of the signal.

Like this FDR is calculated between signals of different classes. In this study, FDR has been calculated between:

- Normal-Systolic
- Normal-Diastolic
- Systolic-Diastolic

Those features are selected which have higher value of FDR.

Also, features have been evaluated. Each feature has been plotted against every feature to see which features are capable of separating the classes. Those features have been selected in which the signals of the three classes were separated out from each other. A total of 378 plots have been made with the help of Microsoft Excel 2007. It is seen that during plotting of features against each other that when we plot the following features, the classes are completely separated and a classification algorithm has been made in MATLAB with the help of these features.

1. Tb v/s RMS1
2. Tb v/s Max1
3. RMS1v/s RMS2
4. Max1 v/s RMS2

4.2.4 Classification

This is the last stage of the methodology. In this stage, the selected features are used to classify the signals into the pre-defined classes. Here the pre-defined classes are normal, systolic murmur and diastolic murmur signal. Classifier is used for the classification. A classifier can be defined as an algorithm which predicts the class label of an object based on its description. The description of the objects is the set of values of the selected feature values relevant for the classification task in the form of a vector. In this study, 3 classifiers were used are listed below.

- ANN (Artificial Neural Network): It is a computational model which is based on structure and function of biological neuron. Information flowing through ANN affects the structure of the network and it changes or we can say it learns based on the input and output.

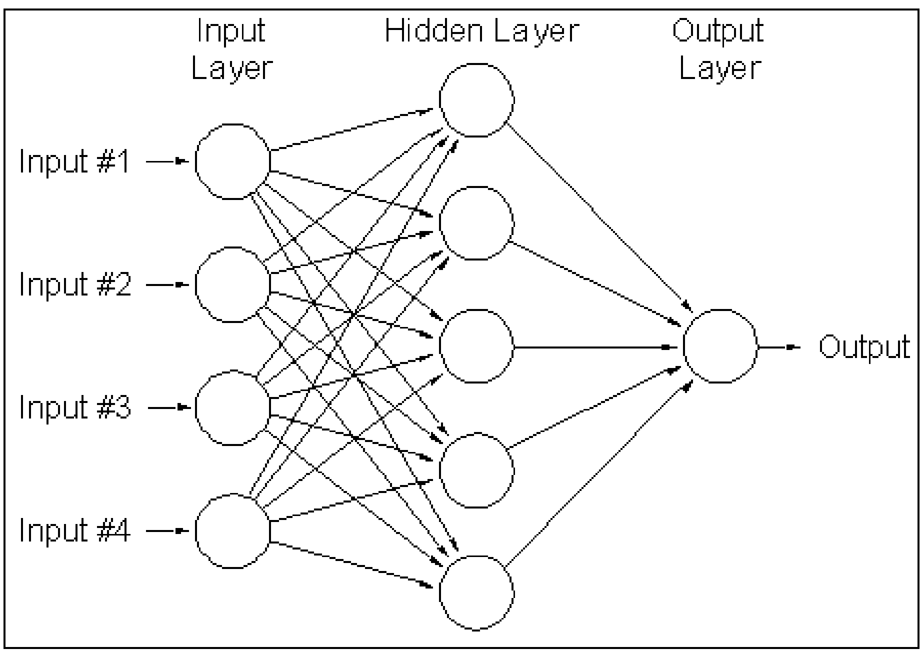

Figure 4.4: A simple multi layer Artificial Neural Network [57].

- k-NN (k- Nearest Neighbor): In k-NN, the object to be classified is given the class label by majority votes from its neighbors. The output of the classification by k-NN is the class membership.

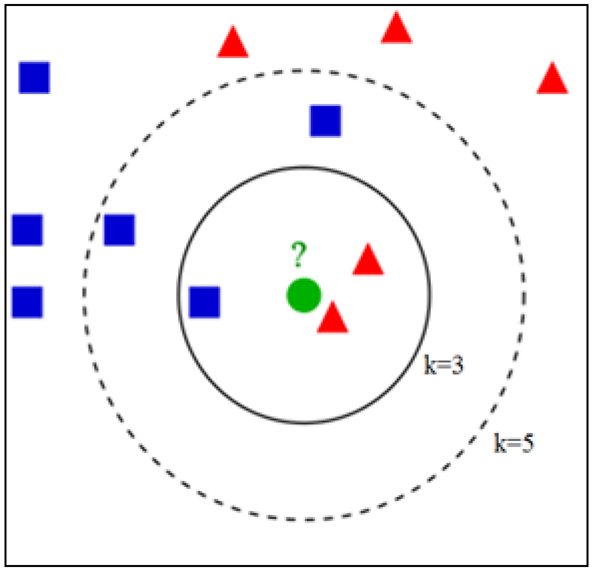

Figure 4.5: Classification by kNN classifier [58].

- Fuzzy k-NN: Class membership is assigned to sample vector (to be classified) instead of assigning it to a particular class. The membership which is assigned to the vector is the function of the vector's distance from its *k*-nearest neighbors and those neighbors' memberships in possible classes.

These classifiers have been applied in MATLAB for classifying the signals. Classification accuracy is then calculated accordingly depending upon how many signals are classified correctly. Also, we have applied adaptive weighted fisher discriminant ratio method for classification [59]. Algorithm for this has been developed in MATLAB.

4.3 Algorithm for Adaptive Weighted Fisher Discriminant Ratio

Step 1: Divide the signals into two sets i.e. training set (94 signals) and test set (50 signals).

Step 2: Calculate mean and standard deviation for selected features of the systolic murmur signals of training set and then calculate the range for each feature.

Step 3: If the value of feature of test sample lies in this range it is classified as the systolic murmur signal otherwise it is either normal signal or diastolic murmur signal.

Step 4: For the selected features, calculate mean (μ_{x1}) and standard deviation (σ_{x1}) for training set for normal class and feature 1.

Step 5: Calculate the range for each selected feature for normal class using mean and standard deviation.

Range = (μ_{x1}- σ_{x1}) to (μ_{x1}+ σ_{x1}) (4.2)

Step 6: Normalized weight is calculated for the selected features using the FDR value.

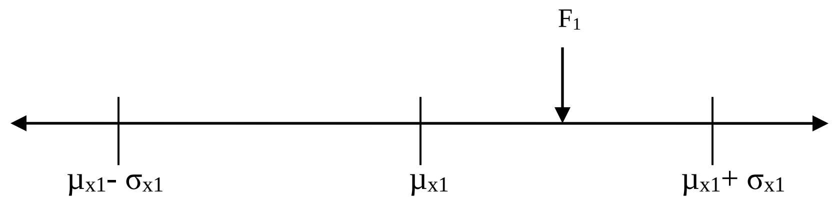

Figure 4.6: The value of feature lying in the range of value.

Step 7: Now, for each sample value normalized weight is calculated to see how near the value lies for the sample value F_1 for one class using the following equation.

$$Z_{x1} = \left(1 - \frac{|\mu_{x1} - F_1|}{\sigma_{x1}}\right) \quad (4.3)$$

Step 8: For normal class, the weighted score WZ_{x1} is calculated for each feature. It is calculated by multiplying the Z_{x1} with its FDR weight.

$WZ_{x1} = Z_{x1}$ X (FDR weight) (4.4)

Step 9: Total weighted score is then calculated by adding the weighted score for all the features for a class WZ_xA.

$$WZ_xA = \sum_{k=1}^{n} WZ_{xk} \quad (4.5)$$

Here, n represents the number of features.

Step 10: The same procedure (steps 6 to 9) are repeated for second class (using the mean and standard deviation of the class from which range is calculated) and WZ_xB is calculated.

Step 11: Difference between WZ_xA and WZ_xB is calculated.

Step 12: Steps 5 to 11 are repeated for diastolic murmur class.

Step 13: Threshold is set according to the difference between the total weighted score difference.

Step 14: If the value of this difference is greater than threshold then signal is classified as normal signal but if the difference is less than threshold the signal is classified as diastolic murmur signal.

CHAPTER 5

RESULTS

PCG signal has the potential to detect heart diseases at an earlier stage. In this study, the signals have been classified into three classes namely normal signal, systolic murmur signal and diastolic murmur signal. The results of this study have been compiled below.

5.1 Feature Evaluation

All the features have been evaluated. Each feature has been plotted against every feature to see which features are capable of separating the classes. Those features have been selected in which the signals of the three classes were separated out from each other.

A total of 378 plots have been made with the help of Microsoft Excel 2007. It is seen that during plotting of features against each other that when we plot the following features, the classes are completely separated and a classification algorithm has been made in MATLAB with the help of these features.

1. Tb v/s RMS1
2. Tb v/s Max1
3. RMS1v/s RMS2
4. Max1 v/s RMS2

Figures 5.1 to 5.4 show the three classes of the signals which have been plotted and are separated out and each class has been encircled to have a better view.

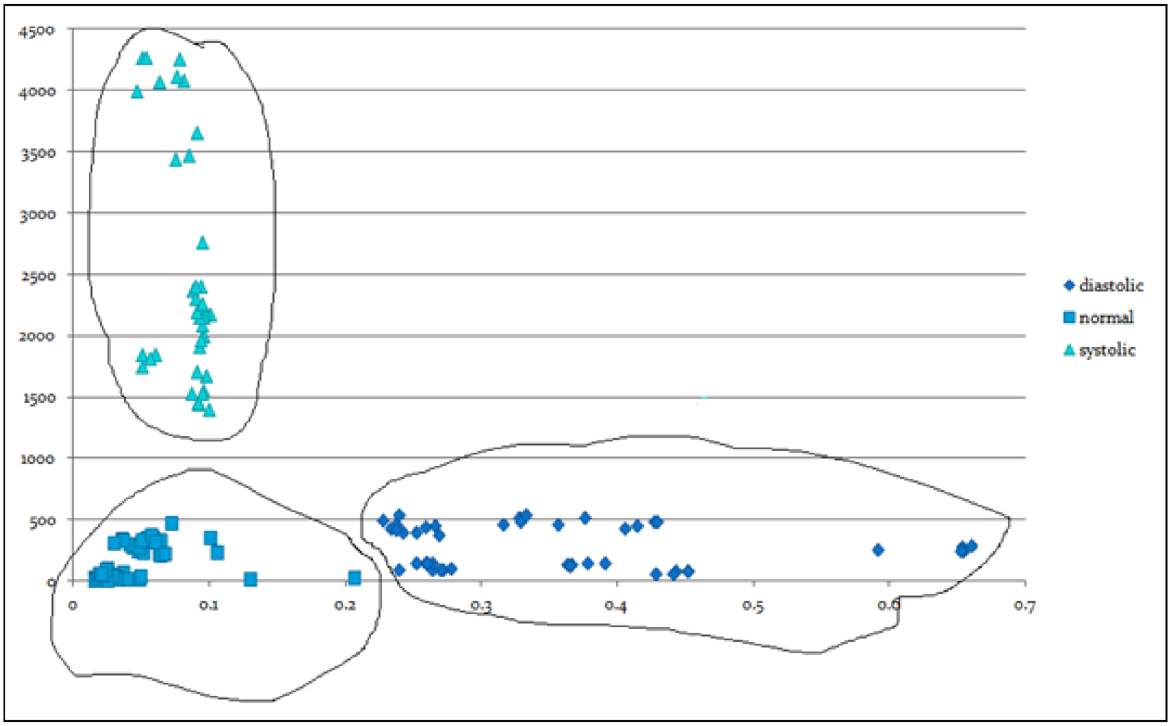

Figure 5.1: Plot between Tb and RMS1.

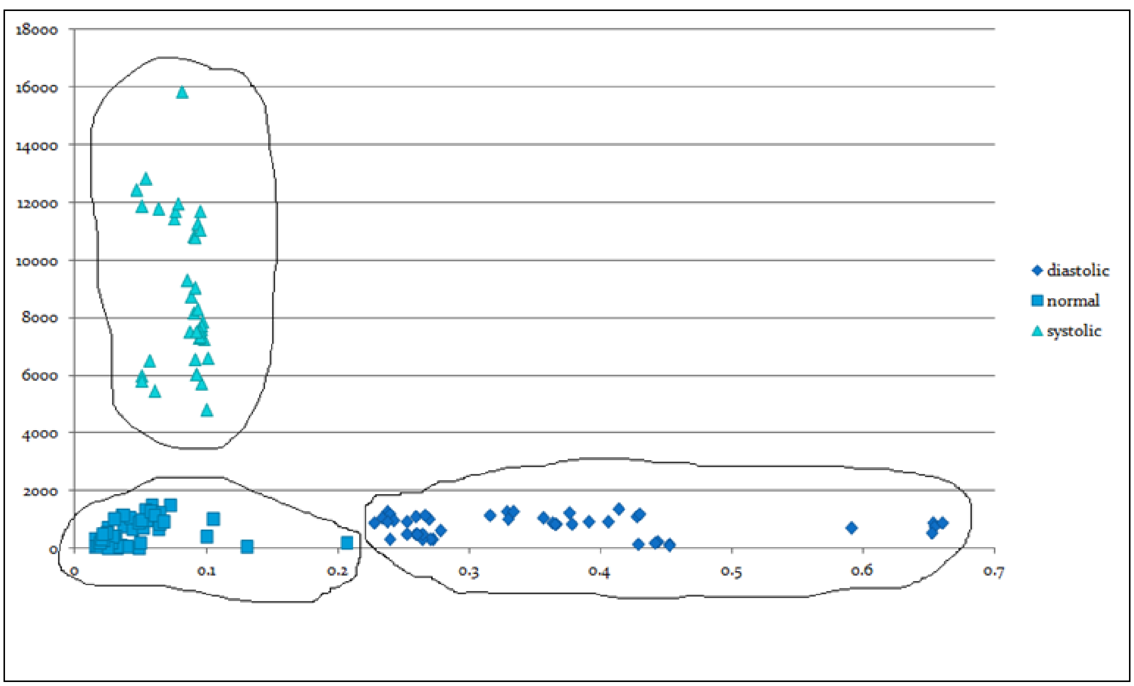

Figure 5.2: Plot between Tb and Max1.

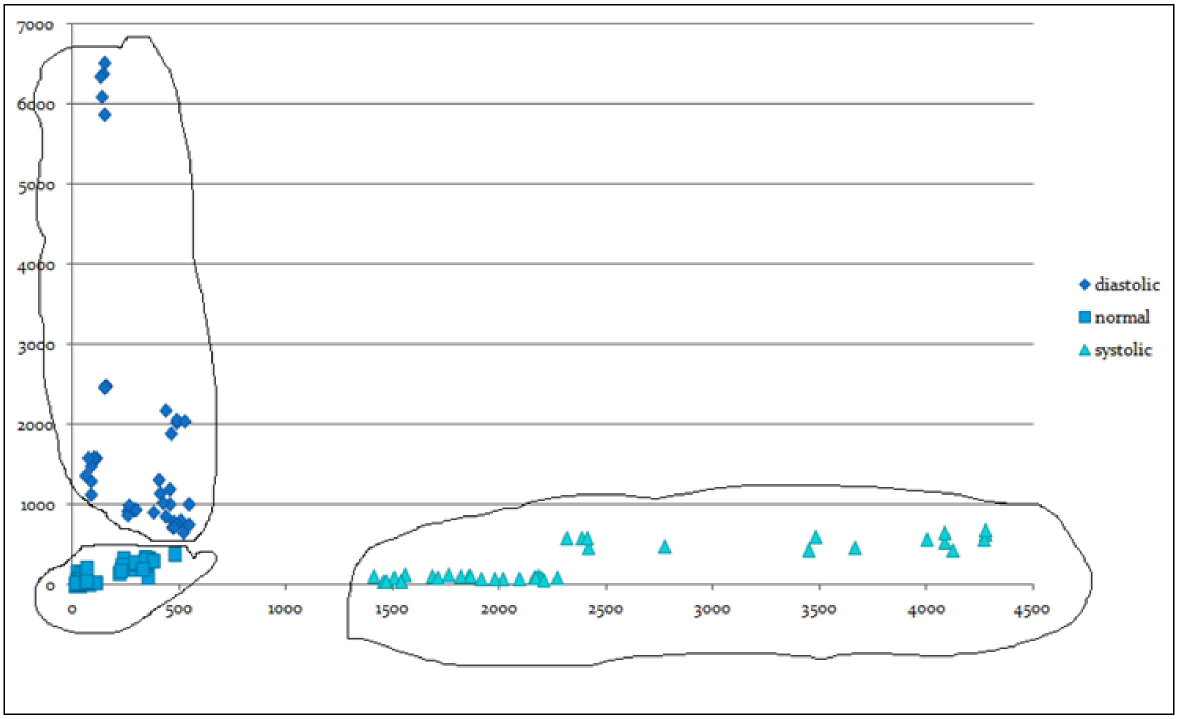

Figure 5.3: Plot between RMS1 and RMS2.

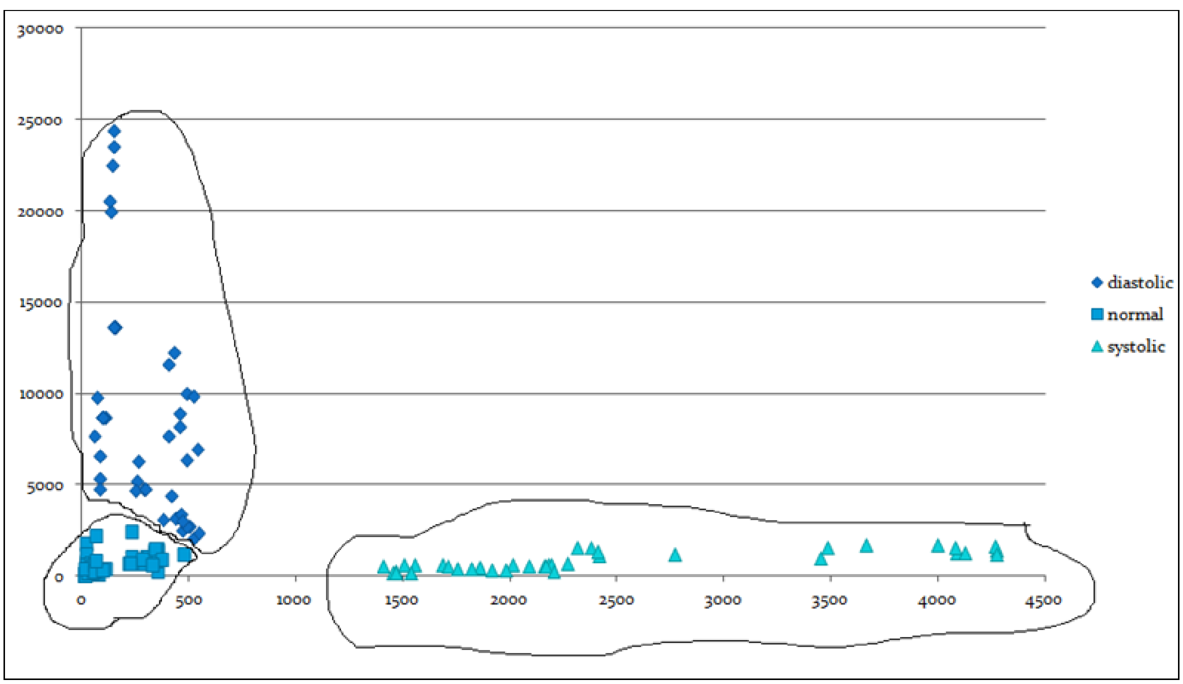

Figure 5.4: Plot between Max1 and RMS2.

5.2 Classification of Signals Using Different Classifiers

Three different classifiers have been used to classify the signal. Out of all the extracted features, only selected features are used for classification. These selected features are given as the input to the classifier. 5 fold cross-validation has been used in this study.

5.2.1 Feature Extraction

Features have been extracted in different domains i.e. time domain, frequency domain and statistical domain as shown in tables 5.1 to 5.12. A total of 28 features have been extracted for each signal. New features like Max1, Max2 are also introduced in this study.

Table 5.1: Time domain features of normal signals.

S. No.	Peak Amp.	Total Power	ZCR	RMS	Ta	Tb
1	-72.65	-59.52	8258.574	212.1702	0.052	0.036
2	-70.74	-59.36	8246.248	196.2314	0.03	0.025
3	-65.38	-56.06	7798.12	195.3813	0.035	0.026
4	-74.43	-60.28	7834.271	239.1783	0.027	0.025
5	-75.97	-60.64	8466.873	241.5989	0.053	0.03
6	-79.8	-65.37	9556.072	170.3104	0.048	0.033
7	-81.8	-65.26	9309.885	128.989	0.07	0.039
8	-82.71	-64.84	9213.847	158.359	0.049	0.031
9	-81.84	-65.05	9413.583	126.3632	0.053	0.03
10	-84.18	-65.21	8938.047	138.5563	0.05	0.048
11	-58.94	-51.01	7334.261	358.8046	0.07	0.026
12	-73.37	-61	7364.089	379.753	0.065	0.026
13	-60.88	-51.16	7065.609	399.6648	0.063	0.034
14	-79.8	-62.75	7572.557	373.8313	0.066	0.032
15	-71	-59.53	7206.612	377.7524	0.075	0.039
16	-76.84	-66.64	4877.574	3061.014	0.255	0.13
17	-71.06	-65.51	5208.065	2647.503	0.145	0.1
18	-73.52	-64.5	6143.501	2637.225	0.176	0.049
19	-41.65	-36.23	4270.187	2677.865	0.155	0.105
20	-81.32	-69.79	4957.257	2998.261	0.229	0.206
21	-87.71	-70.63	10161.21	224.8578	0.062	0.015
22	-86.44	-71.25	11929.95	194.1319	0.053	0.015

S. No.	Peak Amp.	Total Power	ZCR	RMS	Ta	Tb
23	-82.99	-66.16	11856.79	171.0607	0.044	0.015
24	-82.45	-65.85	11016.48	145.3452	0.04	0.019
25	-87	-72.01	11420.07	199.6233	0.039	0.016
26	-73.86	-61.95	10311.44	237.4203	0.049	0.029
27	-76.38	-61.73	10560.78	204.4503	0.045	0.025
28	-74.63	-62.85	11047.93	183.2606	0.059	0.03
29	-74.83	-63.64	10276.66	181.41	0.03	0.018
30	-76.68	-62.19	10805.4	247.0039	0.049	0.029
31	-71.25	-62.59	9386.65	1198.476	0.033	0.031
32	-75.66	-64.64	9293.463	1390.629	0.026	0.024
33	-55.65	-48.17	9050.612	1721.174	0.028	0.027
34	-77.89	-65.99	9924.867	1414.735	0.021	0.028
35	-71.67	-59.77	10299.84	1202.611	0.03	0.024
36	-32.94	-24.97	1483.376	1040.734	0.069	0.047
37	-33.77	-26.09	1321.995	1130.454	0.076	0.043
38	-29.79	-22.05	1328.103	1169.52	0.065	0.041
39	-37.1	-29.55	1187.513	951.4158	0.048	0.035
40	-35.87	-28.16	1442.015	759.438	0.064	0.051
41	-46.2	-37.05	3141.997	875.6911	0.077	0.058
42	-44.73	-36.55	2581.134	935.2621	0.091	0.072
43	-44.73	-37.08	3119.135	1067.688	0.083	0.058
44	-40.32	-33.54	3230.066	1057.331	0.098	0.064
45	-44.59	-36.83	3413.625	853.6308	0.099	0.053
46	-47.34	-37.22	1374.001	945.8564	0.058	0.036
47	-47.77	-37.97	1269.381	617.9472	0.053	0.029
48	-48.9	-37.24	1335.889	795.5061	0.071	0.048
49	-48.18	-37.96	1298.466	947.6247	0.08	0.054
50	-47.61	-36.22	1240.631	1067.239	0.071	0.05
51	-71.33	-58.85	6718.336	1926.796	0.03	0.021
52	-69.19	-58.14	7175.487	1558.797	0.021	0.018
53	-68.25	-58.57	6804.298	1663.39	0.018	0.019
54	-72.3	-59.55	7306.4	1764.434	0.036	0.023
55	-71.45	-59.52	7077.332	1774.086	0.024	0.02
56	-41.98	-36.08	760.0727	1734.655	0.075	0.057
57	-51.4	-43.27	1616.873	1595.46	0.079	0.063

S. No.	Peak Amp.	Total Power	ZCR	RMS	Ta	Tb
58	-51.93	-43.45	1385.885	1566.641	0.074	0.064
59	-52.5	-43.52	1024.906	1673.059	0.069	0.06
60	-49.47	-40.91	1199.487	1578.867	0.072	0.067

Table 5.2: Features extracted in systolic and diastolic regions of normal signals.

S. No.	ZCR1	ZCR2	RMS1	RMS2	Max1	Max2
1	8258.574	9449.134	78.227	24.65885	797	125
2	9018.616	9045.925	26.664	25.59756	125	114
3	8319.839	8663.777	31.161	27.9894	163	161
4	7112.789	9563.822	65.268	24.2128	255	107
5	9473.363	9523.33	25.153	24.08627	130	110
6	10194.05	11364.76	13.904	12.6901	81	70
7	10508.1	10951.36	14.263	13.32371	90	63
8	10171.31	10948.69	15.364	14.25041	71	106
9	10461.2	11270.09	14.877	13.24321	76	90
10	10092.66	10553.92	14.591	14.17748	68	77
11	8441.452	8927.156	28.278	38.61043	159	209
12	8874.516	9300.369	23.063	20.09393	142	101
13	8942.778	7861.2	22.140	179.0929	132	1750
14	8787.833	9470.039	24.688	18.27393	131	80
15	8823.7	9070.778	21.848	27.58664	113	155
16	9137.5	10108.3	14.111	19.07764	95	103
17	4480.986	8892.02	353.839	113.7367	460	286
18	8177.859	9515.598	40.202	163.5215	207	544
19	6590.769	6472.789	235.351	340.2939	1047	1032
20	9577.153	10209.45	29.039	57.24859	208	167
21	8750	13228.9	35.445	7.354902	344	100
22	11754.78	14114.53	14.444	6.387156	74	38
23	12543.44	13387.83	10.480	9.528021	95	114
24	11872.21	12075.54	21.449	66.84863	195	792
25	12057.56	13569.41	13.248	6.925244	104	47
26	9618.745	12696.91	41.621	30.42777	268	411
27	11074.83	12009.14	20.475	90.86346	162	1216
28	10775.74	12490.03	39.803	21.34862	444	318

S. No.	ZCR1	ZCR2	RMS1	RMS2	Max1	Max2
29	9231.399	11823.09	29.558	17.82597	112	146
30	8257.101	14237.18	53.662	19.06347	351	199
31	10434.38	10376.89	20.967	63.4046	103	585
32	9752.606	10395.32	111.377	41.68992	769	388
33	10605.63	9537.384	37.08471	82.47104	207	719
34	10118.13	10970.91	44.90769	41.1939	456	575
35	11415.04	11510.45	13.16979	37.1926	60	414
36	1748.618	2010.96	246.8211	205.9201	809	667
37	1269.876	1879.856	283.814	215.2496	685	703
38	1594.163	1742.251	300.3015	269.8034	1085	1048
39	1371.169	1588.702	344.7167	259.4925	1166	856
40	1909.744	1780.152	233.3931	222.5436	763	674
41	3766.22	3550.52	355.4381	321.539	1515	1511
42	2732.899	3189.053	477.1333	394.6461	1535	1235
43	3629.289	3565.237	355.8494	347.8093	1336	1372
44	3739.162	3592.027	340.176	361.9384	1262	1334
45	3799.298	1297	343.6993	328.2807	1364	1297
46	1426.456	1649.723	330.8578	279.2387	1189	998
47	1386.464	1465.62	311.5617	293.793	1048	1061
48	1397.024	1551.164	285.4668	287.3368	913	899
49	1385.859	1598.166	353.9878	287.9572	1005	926
50	1474.719	1384.096	339.4757	319.167	1032	1488
51	6271.282	8032.289	55.8078	176.571	309	622
52	6322.822	8830.476	59.46609	40.73474	218	248
53	5845.705	8109.574	64.51467	221.057	353	2183
54	5446.361	9508.625	99.86034	42.31349	582	317
55	6135.652	8554.151	67.1902	52.50187	523	814
56	884.4937	862.1995	373.8831	301.5803	1298	876
57	1173.648	2366.942	231.0186	256.6976	698	2436
58	1299.182	1841.326	219.1971	160.512	900	717
59	886.9274	1337.083	328.4167	206.2123	1175	645
60	997.3257	1692.668	226.5827	184.435	976	705

Table 5.3: Frequency domain features of normal signal.

S. No	THD	IMD	Peak Freq.	Peak Freq.(s)	BW(s)	Q Factor (s)	Peak Freq. (p)	BW(p)	Q Factor (p)	Crest factor	Dynamic range
1	153.98	94.667	145.349	145.349	20.801	6.988	156.116	35.602	4.385	20.459	66.99
2	111.98	78.853	188.416	188.416	12.501	15.072	156.116	33.902	4.605	20.837	66.69
3	69.56	53.057	156.116	156.116	29.102	5.364	150.732	35.702	4.222	20.124	65.94
4	197.74	95.05	129.199	129.119	7.9	16.354	156.116	34.602	4.512	21.421	68.99
5	199.46	102.03	188.416	188.416	9.501	19.832	150.732	34.502	4.369	21.118	68.78
6	213.59	59.706	139.966	139.996	9.601	14.579	183.032	71.104	2.574	21.468	66.09
7	258.91	99.661	156.116	156.116	10.101	15.456	183.032	36.502	5.014	21.040	63.25
8	276.28	117.59	177.65	177.65	12.601	14.098	172.22	56.903	3.03	21.905	65.89
9	244.18	89.445	177.649	177.649	28.502	6.233	183.032	21.901	8.357	20.858	62.89
10	126.69	97.976	807.495	807.495	7.698	104.89	166.882	17.301	9.646	19.806	62.64
11	81.02	106.87	48.45	48.45	39.499	1.227	43.066	18.3	2.353	15.805	66.90
12	262.60	135.82	37.683	37.683	23.1	1.631	43.066	16.9	2.548	17.158	68.75
13	45.69	56.67	145.349	145.349	13.301	10.928	43.066	18.9	2.279	15.959	67.99
14	393.37	161.76	59.216	59.216	13.9	4.26	43.066	16.9	2.548	15.967	67.42
15	132.16	101.35	129.199	129.199	6.8	18.999	43.066	15.4	2.797	15.351	66.89
16	147.45	99.813	48.45	48.45	15	3.23	26.917	17.6	1.529	19.443	89.16
17	95.71	128.95	32.3	32.3	9.7	3.33	21.533	23.8	0.905	18.156	86.61
18	204.29	124.42	26.917	26.917	14.2	1.896	21.533	29	0.743	19.194	84.42
19	58.31	83.18	37.683	37.683	11.6	3.249	32.3	25.3	1.277	16.643	85.19
20	195.79	66.46	43.066	43.066	9.2	4.681	26.917	18.6	1.447	19.770	89.31
21	188.86	111.63	258.398	258.398	8.401	30.76	145.349	20.601	7.055	19.397	66.43
22	171.62	56.48	215.332	215.332	13.901	15.491	145.349	25.102	5.79	19.767	65.52
23	183.18	125.95	247.632	247.632	10.601	23.36	145.349	26.802	5.423	22.926	67.58
24	106.83	119.34	376.831	376.831	11.401	33.053	150.732	26.502	5.688	22.362	65.61
25	209.95	54.64	193.799	193.799	7.4	26.187	139.966	21.501	6.51	20.128	66.13
26	150.78	113.06	134.583	134.583	8.701	15.468	113.049	16.5	6.852	20.510	68.02
27	118.74	94.52	253.015	253.015	7.7	32.857	107.666	26.6	4.048	21.470	67.68
28	70.56	74.38	231.482	231.482	8.701	26.605	183.032	30.802	5.942	24.06	61.07
29	92.84	88.76	183.032	183.032	7.1	25.778	118.433	52.101	2.273	21.73	66.91
30	101.39	62.96	328.381	328.381	19.101	17.192	107.666	22.1	4.872	21.336	69.19
31	74.48	54.15	129.199	129.199	10.2	12.666	172.266	79.305	2.172	22.763	84.33
32	135.05	72.26	118.43	118.43	12.4	9.551	172.26	69.004	2.49	21.702	84.56

S. No	THD	IMD	Peak Freq.	Peak Freq.(s)	BW(s)	Q Factor (s)	Peak Freq. (p)	BW(p)	Q Factor (p)	Crest factor	Dynamic range
33	30.91	61.15	113.05	113.05	6.4	17.664	161.49	71.604	2.25	23.133	87.85
34	164.19	78.24	102.28	102.28	10.8	9.471	172.26	78.505	2.19	22.555	85.57
35	73.86	69.39	172.26	172.26	14.101	12.217	172.26	80.405	2	22.453	84.05
36	19.65	50.58	150.73	150.73	17.901	8.42	150.73	17.401	8.66	18.859	79.20
37	18.55	62.17	145.35	145.35	21.501	6.76	107.66	55.101	1.95	18.448	79.51
38	14.32	28.38	139.96	139.96	22.40	6.248	139.96	22.801	6.14	18.175	79.53
39	28.57	63.54	172.26	172.26	11.60	14.85	123.81	47.301	2.62	18.425	77.99
40	73.65	59.02	96.899	96.899	15	6.46	96.899	14.8	6.55	19.40	77.01
41	57.35	86.15	113.05	113.05	17.4	6.497	80.75	19.7	4.09	19.983	78.83
42	66.76	102.62	91.516	91.516	8.9	10.283	86.133	27.2	3.16	19.556	78.97
43	59.85	79.66	107.66	107.66	112.8	0.954	118.43	121.93	0.97	14.788	78.63
44	38.01	74.24	91.516	91.516	20.3	4.508	123.82	18.1	6.84	21.594	82.07
45	43.45	49.69	139.96	139.99	10.40	13.457	86.133	22.4	3.84	20.349	78.97
46	91.72	94.76	161.49	161.49	11.20	14.419	145.35	30.40	4.78	21.756	81.27
47	86.84	91.32	150.73	150.73	11.90	12.66	113.05	32.3	3.5	21.376	77.19
48	129.25	110.23	166.88	166.88	23.70	7.041	166.88	19.00	8.78	21.598	79.61
49	20.62	27.97	619.08	619.08	8.898	69.576	156.12	38.20	4.08	20.653	80.18
50	26.01	26.51	500.64	500.64	8.601	58.211	166.88	26.00	6.42	19.702	80.26
51	124.97	86.21	177.65	177.65	10.60	16.758	274.55	72.60	3.78	24.472	90.16
52	106.86	59.90	161.49	161.49	11.80	13.686	166.88	102.6	1.62	24.655	88.51
53	89.122	63.75	183.03	183.03	9.501	19.265	285.31	100.4	2.84	24.887	89.30
54	118.91	71.58	253.01	253.01	11.20	22.589	253.01	59.70	4.24	25.311	90.24
55	142.62	83.63	150.732	150.732	9.601	15.7	306.848	98.806	3.106	25.123	90.10
56	31.61	42.52	113.049	113.049	12.2	9.266	139.996	57.403	2.438	22.321	87.10
57	66.88	73.72	107.666	107.666	15.2	7.083	134.583	37.502	3.589	22.797	86.85
58	16.74	32.69	161.499	161.499	21.501	7.511	166.882	44.503	3.75	22.809	86.71
59	24.78	44.66	156.116	156.116	21.801	7.161	145.349	59.704	2.435	22.757	87.22
60	25.32	56.86	150.73	150.73	31.10	4.846	139.996	76.503	1.83	22.544	86.51

Table 5.4: Statistical domain features of normal signals.

S. No.	Mean	Standard deviation	Variance	Skewness	Kurtosis
1	-0.753172693	212.1702	45016.19	0.205512	64.27653
2	1.07145645	196.2314	38506.78	-0.08038	91.08622
3	1.252733482	195.3813	38173.83	0.263152	59.25113
4	-0.682699743	239.1783	57206.27	-0.76574	84.57902
5	-1.874173004	241.5989	58370.01	0.126751	87.82034
6	-2.851494581	170.3104	29005.62	-0.35584	97.29164
7	-0.522607596	128.989	16638.17	0.594394	79.5655
8	0.613485368	158.359	25077.58	-0.97915	100.8695
9	1.964861525	126.3632	15967.65	-0.22838	47.8098
10	-0.826538497	138.5563	19197.85	-0.5753	47.58084
11	-6.545229151	358.8046	128740.7	-0.38503	14.0371
12	-0.353697064	379.753	144212.4	0.628471	23.83554
13	1.767957549	399.6648	159732	0.51953	22.52596
14	3.296468627	373.8313	139749.8	0.771706	22.52193
15	4.842741652	377.7524	142696.9	0.527802	19.4891
16	-47.25432865	3061.014	9369807	-1.92848	55.33298
17	-33.29761966	2647.503	7009274	-1.20981	41.78655
18	-15.83185793	2637.225	6954958	-0.57913	29.84462
19	-20.7817403	2677.865	7170962	-0.90713	27.83457
20	-33.19835349	2998.261	8989571	-2.3821	56.75024
21	-0.561662346	224.8578	50561.05	0.097772	68.5369
22	-1.22185538	194.1319	37687.18	0.156707	66.48858
23	0.518735856	171.0607	29261.77	0.525572	127.3722
24	-1.869433908	145.3452	21125.21	0.396197	99.27163
25	-0.804985667	199.6233	39849.45	0.533569	44.412
26	-0.864056452	237.4203	56368.38	0.109294	82.07646
27	3.136410907	204.4503	41799.92	1.184152	88.96867
28	0.57994962	183.2606	33584.44	0.260693	106.1923
29	-0.401909579	181.41	32909.6	-0.08456	118.2423
30	0.008710754	247.0039	61010.95	0.357112	82.7101
31	-0.32919801	1198.476	1436344	0.207784	103.105
32	2.939323255	1390.629	1933850	-0.43876	109.3945
33	-3.148236181	1721.174	2962441	-1.59821	111.9511
34	0.151142752	1414.735	2001475	-0.21549	83.01683

S. No.	Mean	Standard deviation	Variance	Skewness	Kurtosis
35	0.239958981	1202.611	1446273	-0.50682	122.4924
36	4.472217962	1040.734	1083127	-0.39271	28.84361
37	-6.122231581	1130.454	1277926	-0.2585	35.60562
38	-7.634871186	1169.52	1367777	-0.52574	34.85627
39	0.768634556	951.4158	905192	0.265343	30.78919
40	-6.388173793	759.438	576746.1	-0.79218	40.79665
41	2.753591243	875.6911	766835	0.014413	35.2339
42	-6.174202874	935.2621	874715.1	0.518771	32.43742
43	-7.586043788	1067.688	1139958	-0.92865	34.3954
44	-14.43941914	1057.331	1117948	0.991462	61.57487
45	-9.783055575	853.6308	728685.5	-0.28984	47.00456
46	-2.100310431	945.8564	894644.3	-1.00868	81.86148
47	-5.491154009	617.9472	381858.8	-1.54642	45.40867
48	2.001856167	795.5061	632830	-1.07539	75.84008
49	-1.461821563	947.6247	897992.6	-0.72361	63.54316
50	-3.915135945	1067.239	1139000	-0.68481	53.75559
51	9.665327463	1926.796	3712543	0.857156	197.6346
52	0.771252354	1558.797	2429849	1.156186	237.4637
53	2.078367751	1663.39	2766865	-0.38236	229.3725
54	9.233805472	1764.434	3113228	3.164221	145.5445
55	3.109160889	1774.086	3147382	0.23077	240.1918
56	-1.791613898	1734.655	3009028	0.773377	84.14518
57	-4.852680808	1595.46	2545492	1.346602	102.7348
58	4.064070561	1566.641	2454363	0.812894	94.94495
59	-1.476622949	1673.059	2799128	0.444863	127.1135
60	-5.557149443	1578.867	2492820	0.995863	122.906

Table 5.5: Time domain features of diastolic signals.

S. No.	Peak Amp.	Total Power	ZCR	RMS	Ta	Tb
1	-36.93	-34.89	199.2581	3515.28	0.086	0.269
2	-42.5	-39.1	210.3675	3502.764	0.085	0.259
3	-46.69	-40.09	287.233	3478.96	0.083	0.228
4	-35.09	-33.78	217.2652	3460.553	0.087	0.237
5	-44.24	-40.93	197.0747	3460.927	0.09	0.233
6	-44.97	-40.42	227.0258	3110.448	0.101	0.328
7	-45.28	-40.97	365.9589	3110.606	0.108	0.356
8	-43.13	-38.7	233.0519	3100.536	0.111	0.329
9	-48.33	-42.61	257.5125	3115.927	0.087	0.316
10	-44.58	-40.09	250.4953	3136.228	0.082	0.333
11	-48.13	-41.3	276.5678	3110.898	0.088	0.252
12	-47.57	-41.85	248.561	3201.662	0.072	0.266
13	-46.25	-40.79	257.4743	3174.813	0.093	0.239
14	-45.09	-40.42	227.0662	3155.594	0.081	0.242
15	-44.81	-41.77	266.815	3164.767	0.091	0.237
16	-29.06	-25.63	234.0465	3735.795	0.082	0.406
17	-28.32	-25.12	234.8426	3646.601	0.086	0.427
18	-30.53	-25.64	234.9046	3652.105	0.081	0.429
19	-29.73	-26.65	299.9088	3630.882	0.081	0.414
20	-28.84	-26.92	226.7195	3641.314	0.078	0.376
21	-21.53	-12.7	328.9352	6541.093	0.134	0.366
22	-20.64	-12.74	329.9095	6604.112	0.132	0.378
23	-22.73	-13.3	354.8362	6342.233	0.121	0.363
24	-23.11	-13.02	335.7551	6283.414	0.136	0.391
25	-23.24	-12.73	365.6089	6511.358	0.134	0.365
26	-56.98	-45.4	1383.44	1081.057	0.063	0.653
27	-58.41	-45.77	1269.425	1050.971	0.055	0.654
28	-56.39	-45.2	1375.035	1005.203	0.043	0.652
29	-56.55	-44.29	1331.905	1089.612	0.046	0.591
30	-56.98	-45.4	1383.44	1081.057	0.045	0.66
31	-60.8	-48.52	1769.93	1314.828	0.07	0.278
32	-60.92	-48.54	1780.271	1310.19	0.062	0.272
33	-61.43	-48.62	1768.049	1315.25	0.066	0.27
34	-59.72	-48.69	1763.336	1337.179	0.053	0.264

S. No.	Peak Amp.	Total Power	ZCR	RMS	Ta	Tb
35	-60.92	-48.54	1774.622	1315.081	0.052	0.239
36	-56.66	-44.74	1797.079	2075.849	0.075	0.264
37	-56.5	-44.75	1813.219	2068.769	0.066	0.259
38	-56.73	-44.74	1808.392	2068.916	0.071	0.252
39	-56.5	-44.75	1805.048	2075.718	0.067	0.26
40	-57.47	-44.66	1827.922	2052.663	0.07	0.26
41	-52.81	-40.36	456.6451	1581.201	0.06	0.452
42	-52.85	-42.01	465.7565	1476.632	0.057	0.452
43	-53.59	-42.72	522.4905	1458.874	0.054	0.443
44	-49.9	-39.88	483.4481	1648.84	0.051	0.441
45	-50.26	-43.07	468.736	1561.148	0.057	0.428

Table 5.6: Features extracted in systolic and diastolic regions of diastolic murmur signals.

S. No.	ZCR1	ZCR2	RMS1	RMS2	Max1	Max2
1	191.5559	235.0564	373.4479	912.6458	1020	3173
2	383.9946	142.445	448.522	1014.256	1136	3267
3	322.2172	342.4103	497.5402	825.094	912	2813
4	296.2183	208.4872	466.0435	800.0391	1314	2593
5	240.0653	209.7445	431.1505	870.3884	1088	3243
6	85.04132	323.8318	514.3641	671.0284	1276	2139
7	225.6048	500.2469	460.9568	731.1891	1070	3450
8	256.012	248.0087	484.1499	758.7871	1043	2756
9	187.8594	330.5139	465.4891	734.3857	1164	3069
10	137.2169	330.5285	541.4855	771.372	1304	2395
11	171.9755	357.7627	402.1277	1148.451	949	7712
12	169.4487	307.3057	452.3425	1212.95	1171	8247
13	137.1932	341.3055	536.3904	1015.902	1192	7035
14	250.5901	244.2623	399	1330.665	1000	11654
15	138.2445	353.421	416.9179	1031.82	965	4429
16	102.2381	349.284	429.8498	2191.433	925	12304
17	151.3977	308.0326	484.3445	2045.893	1100	6408
18	165.6679	319.3119	484.3967	2072.487	1219	10049
19	338.8894	340.1207	455.0566	1900.65	1381	8950
20	120.6282	322.7223	519.5299	2048.643	1247	9905

S. No.	ZCR1	ZCR2	RMS1	RMS2	Max1	Max2
21	647.0426	295.9732	139.5971	6404.472	864	22572
22	671.8281	266.7339	143.5378	6534.21	843	24453
23	759.8101	268.3513	133.7395	6108.656	915	20001
24	622.4202	328.3693	143.8456	5885.668	957	23550
25	932.9243	229.9796	123.4906	6372.539	858	20592
26	1569.395	1466.757	284.3457	958.0551	903	4796
27	1347.884	1345.074	250.6635	929.943	772	5240
28	1382.673	1477.288	249.2398	887.0661	570	4731
29	1490.872	1393.827	259.1892	996.2167	744	6321
30	1510.039	1466.757	293.1592	958.0788	903	4796
31	2403.225	1652.202	104.4374	1603.303	628	8760
32	2466.61	1672.987	94.24045	1587.436	322	8759
33	2469.845	1661.595	94.0672	1589.557	322	8762
34	2443.194	1638.213	93.85411	1599.99	320	8761
35	2477.106	1643.801	93.90004	1598.54	322	8759
36	2522.356	1689.181	147.9427	2504.879	504	13684
37	2586.521	1711.878	146.422	2480.392	502	13695
38	2537.514	1697.347	148.195	2490.483	504	13685
39	2568.162	1679.141	147.8627	2498.682	502	13695
40	2558.893	1721.596	146.6081	2486.455	504	13685
41	205.3753	621.5888	81.76689	1491.068	181	5402
42	255.8249	604.6603	82.30522	1309.811	136	6639
43	253.229	700.3905	81.24479	1144.817	251	4837
44	226.7352	642.9097	66.62055	1603.636	217	9875
45	173.8735	652.5841	57.58999	1371.691	143	7748

Table 5.7: Frequency domain features of diastolic murmur signal.

S. No	THD	IMD	Peak Freq.	Peak Freq.(s)	BW (s)	Q Factor (s)	Peak Freq. (p)	BW (p)	Q Factor (p)	Crest factor	Dynamic range
1	120.46	144.14	21.53	59.21	13.3	4.45	32.3	35.2	0.918	15.11	86.03
2	149.58	130.4	21.53	172.26	11.1	15.52	32.3	32.1	1.006	14.83	85.72
3	57.52	110.65	53.83	58.83	14	3.84	32.3	35.7	0.905	18.58	89.41
4	113.45	114.21	21.53	64.6	14.6	4.42	43.066	39.2	1.099	14.63	85.41
5	158.39	147.18	21.53	59.21	14.1	4.2	43.066	35	1.23	14.93	85.71
6	185.35	131.54	21.53	64.6	23.3	2.77	37.683	42.19	0.893	15.66	85.51
7	186.47	115.75	21.53	64.6	8.6	7.51	37.683	41.19	0.915	15.86	85.72
8	147.10	122.59	21.53	64.6	17.1	3.77	43.066	41.59	1.035	15.73	85.56
9	318.97	142.84	16.15	64.6	9	7.17	37.683	41.3	0.912	15.51	85.38
10	234.51	120.45	16.15	59.21	15.7	3.77	37.683	40	0.942	15.72	85.65
11	75.16	95.47	53.83	53.83	8.4	6.41	43.066	39.3	1.096	16.31	86.17
12	211.28	145.82	21.53	53.83	18.1	2.97	37.683	43.99	0.856	15.39	85.50
13	198.42	146.11	21.53	183.03	8.50	21.53	37.683	44.99	0.837	16.75	86.78
14	165.30	128.55	21.53	118.43	22.4	5.28	37.683	42.2	0.893	15.60	85.58
15	159.01	117.20	21.53	64.6	14.9	4.33	37.683	42.1	0.895	15.7	85.71
16	0.98	18.64	188.4	188.41	9.80	19.25	32.3	35.5	0.91	15.36	86.81
17	1.13	16.52	188.4	188.41	9.90	19.03	32.3	31.7	1.019	14.33	85.57
18	1.02	20.01	188.4	188.41	10.5	17.94	32.3	37.1	0.871	14.45	85.70
19	0.93	26.15	188.4	188.41	9.80	19.22	37.683	36.3	1.038	14.45	85.65
20	0.78	36.08	188.4	188.41	8	23.55	32.3	31.9	1.013	14.49	85.72
21	12.02	17.38	67.29	67.29	2.6	25.88	67.291	2.6	25.88	11.32	78.09
22	12.31	34.08	67.29	67.29	2.6	25.88	67.291	2.6	25.88	11.36	78.22
23	24.99	63.13	49.79	49.79	2.7	18.44	49.796	2.7	18.44	11.17	77.67
24	47.77	68.67	49.79	49.79	2.5	19.91	49.796	2.5	19.91	11.47	77.89
25	15.68	69.83	64.6	64.6	2.6	24.84	64.6	2.6	24.84	11.11	77.84
26	132.69	91.22	183.0	183.03	9.6	19.06	172.26	15.0	11.48	16.91	77.59
27	113.06	75.92	242.2	242.25	11.7	20.70	193.79	13.1	14.79	16.62	77.06
28	117.09	67.17	183.0	183.03	7.8	23.46	193.79	12.5	15.50	16.91	76.96
29	233.69	125.42	75.36	113.05	8.9	12.70	134.58	9.0	14.95	15.89	76.64
30	132.69	91.22	183.0	183.03	9.6	19.06	172.26	15.0	11.48	16.91	77.59
31	176.68	121.13	118.4	118.43	14.8	8.0	193.79	21.2	9.14	16.47	78.85
32	177.91	120.41	118.4	118.43	14.9	7.94	193.79	21.6	8.97	16.50	78.84

S. No	THD	IMD	Peak Freq.	Peak Freq.(s)	BW (s)	Q Factor (s)	Peak Freq. (p)	BW (p)	Q Factor (p)	Crest factor	Dynamic range
33	145.09	82.70	183.0	183.03	8.1	22.59	193.79	26.5	7.31	16.47	78.85
34	123.42	79.18	183.0	183.03	8.2	22.32	193.79	9.3	20.83	16.32	78.85
35	177.91	120.41	183.0	118.43	14.9	7.94	193.79	21.6	8.97	16.46	78.84
36	133.75	80.72	183.0	183.03	7.6	24.08	193.79	26.0	7.45	16.37	82.72
37	131.99	79.94	183.0	183.03	7.6	24.08	193.79	13.0	14.90	16.41	82.73
38	134.43	81.03	183.0	183.03	7.7	23.76	193.79	26.0	7.45	16.40	82.72
39	131.99	79.94	183.0	183.03	7.6	24.08	193.79	13.0	14.90	16.38	82.73
40	186.41	117.35	118.4	118.43	15.5	7.64	193.79	27.10	7.15	16.47	82.72
41	31.10	67.91	344.5	344.53	23.5	14.66	123.81	135.7	0.91	15.38	79.37
42	114.82	80.65	118.4	118.43	9.6	12.33	118.43	133.3	0.88	15.91	79.31
43	20.53	49.28	344.5	344.53	22.9	15.04	118.43	132.9	0.89	15.97	79.27
44	6.15	33.78	430.6	430.66	26.4	16.31	123.81	135.7	0.91	15.69	80.05
45	7.97	32.82	392.9	392.98	17.0	23.11	123.81	135.3	0.91	15.32	79.20

Table 5.8: Statistical domain features of diastolic murmur signals.

S. No.	Mean	Standard deviation	Variance	Skewness	Kurtosis
1	36.40990099	3515.28	12357193	-0.05944	12.56055
2	-10.02653194	3502.764	12269355	-0.02235	18.3566
3	-4.539726784	3478.96	12103162	-0.17843	15.98625
4	1.535128774	3460.553	11975430	-0.17238	19.52663
5	-31.00529115	3460.927	11978012	-0.07808	17.77311
6	5.770597018	3110.448	9674889	-0.13348	23.73598
7	18.82873308	3110.606	9675873	-0.14062	21.46735
8	19.6144721	3100.536	9613325	-0.05667	23.96535
9	16.82758776	3115.927	9709004	-0.19024	24.04454
10	-13.38749497	3136.228	9835926	-0.13193	24.41778
11	12.18438768	3110.898	9677689	-0.32648	25.07159
12	10.16007633	3201.662	10250639	-0.1318	20.29495
13	1.765741353	3174.813	10079440	-0.10088	18.68625
14	4.193201828	3155.594	9957773	-0.23459	23.54751
15	0.218492816	3164.767	10015751	-0.18754	21.44761
16	1.322645179	3735.795	13956166	-0.21101	15.36073

S. No.	Mean	Standard deviation	Variance	Skewness	Kurtosis
17	4.070341251	3646.601	13297696	-0.25659	12.04854
18	23.97240161	3652.105	13337871	-0.09775	15.043
19	15.36462653	3630.882	13183301	-0.27213	14.90122
20	-12.56802645	3641.314	13259169	-0.13376	14.69696
21	73.40793234	6541.093	42785897	-0.03522	4.75434
22	71.31706485	6604.112	43614290	0.045378	5.409168
23	72.28485331	6342.233	40223915	-0.0732	3.591235
24	73.25243378	6283.414	39481296	-0.12083	5.651991
25	72.6983764	6511.358	42397781	-0.0233	4.628033
26	-25.27524985	1081.057	1168684	-0.30908	11.99832
27	-25.03292697	1050.971	1104541	-0.19573	11.47346
28	-25.28035593	1005.203	1010433	-0.23743	12.37842
29	-25.40165322	1089.612	1187254	-0.10858	10.25522
30	-25.27524985	1081.057	1168684	-0.23551	11.32441
31	-16.36638049	1314.828	1728774	-0.05698	14.07444
32	-16.26685761	1310.19	1716598	-0.08741	13.72315
33	-16.37865909	1315.25	1729881	-0.15297	39.21351
34	-14.97335969	1337.179	1788047	-0.14863	13.88359
35	-16.3378928	1315.081	1729438	-0.05443	14.36817
36	-25.38118307	2075.849	4309149	-0.10944	14.10208
37	-24.92617233	2068.769	4279805	-0.05299	14.99804
38	-25.19871987	2068.916	4280413	-0.13972	13.71343
39	-24.96092428	2075.718	4308603	-0.08672	14.76549
40	-25.27701861	2052.663	4213427	-0.04173	15.3279
41	-87.44974676	1581.201	2500198	-0.00763	13.17909
42	-86.32782847	1476.632	2180443	0.159224	12.24855
43	-87.77084088	1458.874	2128313	-0.06601	16.82215
44	-87.87997749	1648.84	2718672	-0.13683	12.38838
45	-88.13074875	1561.148	2437183	0.078216	14.4371

Table 5.9: Time domain features of systolic murmur signals.

S. No.	Peak Amp.	Total Power	ZCR	RMS	Ta	Tb
1	-44.66	-40.63	241.2033	3789.709	0.283	0.095
2	-44.64	-39.55	220.9682	3778.859	0.272	0.094
3	-43.13	-38.67	183.153	3745.435	0.267	0.088
4	-39.92	-37.83	207.9202	3706.228	0.277	0.09
5	-42.21	-38.93	199.9093	3742.676	0.272	0.09
6	-39.88	-37.65	282.1189	3650.706	0.376	0.085
7	-43.24	-40.38	364.1302	3698.743	0.369	0.091
8	-42.17	-37.01	245.9548	3640.866	0.367	0.075
9	-43.26	-39.58	244.9504	3853.309	0.365	0.081
10	-37.04	-34.91	206.8415	3860.131	0.361	0.076
11	-37.08	-35.38	246.578	4187.667	0.348	0.047
12	-36.06	-34.7	197.8204	4359.093	0.341	0.05
13	-38.53	-37.61	279.2457	4273.46	0.35	0.078
14	-40.73	-36.7	242.4215	4279.329	0.352	0.053
15	-36.97	-36.7	211.3281	4240.421	0.335	0.063
16	-25.55	-36.7	939.8901	5304.716	0.202	0.096
17	-25.42	-36.7	992.8992	5346.411	0.194	0.098
18	-25.13	-36.7	1043.293	5255.781	0.208	0.1
19	-25.32	-36.7	848.752	5255.996	0.206	0.463
20	-25.22	-36.7	1039.553	5287.256	0.204	0.091
21	-25.01	-36.7	599.8897	4938.196	0.313	0.101
22	-24.95	-36.7	622.1556	5006.328	0.314	0.097
23	-25.04	-36.7	690.0121	5039.207	0.311	0.096
24	-25.03	-36.7	617.3594	5035.911	0.309	0.096
25	-25.23	-36.7	631.7207	5038.27	0.311	0.095
26	-25.49	-36.7	842.8281	5327.458	0.32	0.093
27	-25.63	-36.7	807.9817	5306.895	0.32	0.091
28	-25.22	-36.7	796.002	5269.131	0.331	0.095
29	-25.2	-36.7	826.6871	5229.335	0.326	0.093
30	-25.21	-36.7	777.769	5216.336	0.32	0.094
31	-29.17	-36.7	820.3538	3546.745	0.324	0.087
32	-28.87	-36.7	841.9722	3489.868	0.316	0.092
33	-28.81	-36.7	775.3274	3598.124	0.317	0.095
34	-28.93	-36.7	834.5468	3528.868	0.317	0.092

S. No.	Peak Amp.	Total Power	ZCR	RMS	Ta	Tb
35	-29.23	-36.7	817.0863	3516.395	0.315	0.092
36	-59.8	-36.7	1475.862	1412.449	0.299	0.05
37	-58.45	-36.7	1494.96	1408.917	0.291	0.05
38	-56.97	-36.7	1550.457	1350.78	0.285	0.06
39	-58.18	-36.7	1617.242	1410.029	0.302	0.056

Table 5.10: Features extracted in systolic and diastolic regions of systolic murmur signals.

S. No.	ZCR1	ZCR2	RMS1	RMS2	Max1	Max2
1	309.9734	270.8812	2773.741	484.3855	11729	1190
2	411.1991	160.1662	2414.906	474.8092	7630	1168
3	274.5493	168.8668	2381.439	595.6839	8770	1575
4	300.3165	192.3162	2311.975	585.8194	10858	1553
5	386.119	121.0209	2407.821	584.5764	8179	1336
6	362.659	279.4566	3481.878	599.2633	9324	1596
7	358.8669	1716	3663.049	474.2641	10795	1716
8	369.2093	230.4564	3449.719	432.0714	11477	957
9	356.9183	223.3732	4085.62	529.9313	15866	1296
10	368.068	156.6128	4124.496	433.6936	11719	1250
11	346.2252	176.0951	3999.858	576.2635	12449	1701
12	367.625	118.8158	4272.572	632.6328	11907	1439
13	363.1765	299.5216	4268.096	567.3339	11978	1666
14	366.4921	209.2054	4275.615	689.4625	12839	1194
15	354.8701	152.9248	4081.587	655.6161	11811	1540
16	944.7524	1413.678	1556.753	124.9596	5739	594
17	1085.431	1484.079	1682.223	107.7123	7266	615
18	1220.671	1431.446	1411.624	106.7401	4851	564
19	972.4023	1235.56	1506.757	100.1536	8550	630
20	1038.869	1582.755	1708.369	88.14818	6585	573
21	392.3938	1007.856	2178.249	108.9	6624	600
22	422.1385	1066.286	2190.707	96.12713	7902	618
23	529.961	1163.734	2010.949	84.68875	7608	591
24	422.515	1048.336	2160.206	87.62494	7731	570
25	406.6961	1084.236	2090.125	84.1201	7521	579
26	481.0909	1528.446	2164.048	90.12433	11274	549

S. No.	ZCR1	ZCR2	RMS1	RMS2	Max1	Max2
27	571.3845	1533.38	2202.917	69.33212	9045	285
28	594.0411	1373.876	2266.802	98.84442	11061	675
29	571.3532	1535.582	1914.928	74.3615	8337	309
30	564.708	1358.475	1977.188	77.45906	7326	324
31	544.3737	1579.257	1538.473	45.80866	7516	198
32	570.2586	1495.358	1467.168	49.1031	6030	290
33	620.6823	1460.662	1535.142	48.56606	7374	190
34	490.227	1571.188	1454.331	46.34102	7516	198
35	568.299	1514.504	1464.703	46.7282	6030	190
36	592.0321	2448.076	1757.163	126.4147	6009	429
37	549.6522	2509.712	1855.624	111.2484	5831	384
38	736.3478	2478.422	1859.052	114.9877	5503	505
39	632.3932	2770.06	1817.089	114.2928	6546	374

Table 5.11: Frequency domain features of systolic murmur signal.

S. No	THD	IMD	Peak Freq.	Peak Freq.(s)	BW (s)	Q Factor (s)	Peak Freq. (p)	BW (p)	Q Factor (p)	Crest factor	Dynamic range
1	191.80	128.27	21.53	64.6	21.4	3.019	37.683	37.7	1	14.0906	85.66
2	307.28	131.43	16.15	64.6	8.2	7.878	32.3	34.3	0.942	14.2043	85.75
3	174.66	146.75	21.53	188.416	11.1	16.973	37.683	36.2	1.041	14.1351	85.60
4	190.45	117.66	16.15	53.833	8.4	6.409	37.683	39.9	0.944	14.333	85.71
5	159.37	125.43	21.53	188.416	10.8	17.445	32.3	31.7	1.019	14.25	85.71
6	191.43	136.3	16.15	53.833	6.3	8.545	43.006	36.2	1.19	14.374	85.62
7	148.36	147.32	21.53	59.216	11.3	5.24	37.683	44.599	0.845	14.3126	85.67
8	143.69	105.30	21.53	118.433	16.4	7.222	37.683	42.299	0.891	14.8636	86.08
9	218.03	133.66	16.15	172.266	11.2	15.38	37.683	43.199	0.872	13.8853	85.60
10	114.58	108.92	21.53	64.6	7.4	8.73	37.683	40	0.942	14.0895	85.82
11	180.07	34.57	16.15	80.75	15	5.768	43.066	40.9	1.053	13.453	85.89
12	131.54	122.27	21.53	188.416	10.5	17.943	32.3	31.7	1.019	13.0074	85.79
13	124.54	116.33	21.53	64.6	6.8	9.5	37.683	37.2	1.013	13.6343	86.24
14	149.86	131.10	21.53	86.133	15.9	5.417	37.683	36.1	1.044	13.4026	86.03
15	138.34	129.84	21.53	188.416	12.7	14.835	32.3	34.8	0.928	13.2534	85.80
16	38.99	66.55	43.06	43.066	12.6	3.418	43.066	12.6	3.418	13.5549	78.50

S. No	THD	IMD	Peak Freq.	Peak Freq.(s)	BW (s)	Q Factor (s)	Peak Freq. (p)	BW (p)	Q Factor (p)	Crest factor	Dynamic range
17	38.39	66.23	43.06	43.066	12.2	3.53	43.066	12.2	3.53	13.524	78.543
18	39.38	65.78	43.06	43.066	11.6	3.713	43.066	11.6	3.713	13.6519	78.522
19	39.42	65.50	43.06	43.066	11.8	3.65	43.066	11.8	3.65	13.6102	78.481
20	40.99	65.22	43.06	43.066	11.8	3.65	43.066	11.8	3.65	13.6401	78.562
21	46.90	60.38	47.10	47.104	12.4	3.799	47.104	12.4	3.799	13.3547	77.684
22	40.24	63.70	47.10	47.104	12.8	3.68	47.104	12.8	3.68	13.2573	77.706
23	41.64	61.58	47.10	47.104	13.1	3.596	47.104	13.1	3.596	13.2613	77.767
24	43.81	62.364	47.10	47.104	13	3.623	47.104	13	3.623	13.2659	77.765
25	38.02	63.206	47.10	47.104	15.6	3.02	47.104	15.6	3.02	13.2492	77.753
26	57.81	70.408	43.06	43.066	12	3.589	43.066	12	3.589	13.565	78.553
27	52.78	69.346	43.06	43.066	12.1	3.599	43.066	12.1	3.599	13.4548	78.409
28	55.81	68.34	43.06	43.066	11.5	3.745	43.066	11.5	3.745	13.5926	78.485
29	48.35	68.496	43.06	43.066	11.5	3.745	43.066	11.5	3.745	13.5712	78.398
30	52.44	65.263	43.06	43.066	9.2	4.681	43.066	9.2	4.681	13.6615	78.467
31	58.00	70.592	43.06	43.066	12.4	3.473	43.066	12.4	3.473	13.577	78.553
32	52.15	68.942	43.06	43.066	11.6	3.713	43.066	11.6	3.713	13.5736	78.409
33	55.84	68.55	43.06	43.066	11.6	3.713	43.066	11.6	3.713	13.3841	78.485
34	57.70	70.314	43.06	43.066	11.8	3.65	43.066	11.8	3.65	13.6209	78.553
35	52.94	69.444	43.06	43.066	12.3	3.501	43.066	12.3	3.501	13.5079	78.409
36	170.69	104.408	183.0	183.032	9.90	18.487	193.799	9.601	20.186	15.1582	78.159
37	123.80	70.347	242.2	242.249	7	34.605	193.799	10.301	18.814	14.3892	77.368
38	119.55	72.705	204.5	204.565	10.8	18.94	193.799	10.001	19.379	13.3901	76.003
39	131.67	82.771	177.6	177.649	11.6	15.314	193.799	11.801	16.423	15.2104	78.196

Table 5.12: Statistical domain features of systolic murmur signals.

S. No.	Mean	Standard deviation	Variance	Skewness	Kurtosis
1	-23.0024308	3789.709	14361893	-0.14903	13.04233
2	-12.01848497	3778.859	14279777	-0.16814	10.46446
3	8.934823144	3745.435	14028286	-0.12039	15.06038
4	-2.5899403	3706.228	13736125	-0.10998	14.77896
5	24.59812449	3742.676	14007625	-0.22644	15.67672
6	-5.074982168	3650.706	13327655	-0.10316	13.18164

S. No.	Mean	Standard deviation	Variance	Skewness	Kurtosis
7	10.94251441	3698.743	13680700	-0.11261	11.30273
8	-4.704123457	3640.866	13255902	-0.17926	14.15541
9	-2.558151563	3853.309	14847987	-0.1922	12.34369
10	16.9335934	3860.131	14900614	-0.02957	10.1174
11	6.717645124	4187.667	17536555	-0.04178	9.686283
12	-2.584478693	4359.093	19001688	-0.11663	8.276034
13	6.127638303	4273.46	18262462	-0.20671	0.447386
14	-0.285840561	4279.329	18312660	-0.15267	9.093957
15	-12.637321	4240.421	17981168	-0.06178	8.918397
16	58.11503509	5304.716	28140010	0.010292	12.76527
17	58.67594089	5346.411	28584108	-0.03999	12.41864
18	59.27492652	5255.781	27623231	0.100031	12.17421
19	59.10835702	5255.996	27625498	0.105696	12.14044
20	59.38548497	5287.256	27955077	0.063435	11.22203
21	70.52222599	4938.196	24385776	-0.0127	10.82913
22	71.14060537	5006.328	25063320	-0.07215	10.80247
23	71.04271443	5039.207	25393602	0.011498	12.72554
24	70.22752357	5035.911	25360401	-0.02484	10.36309
25	79.92306798	5038.27	25384168	0.002101	10.62708
26	60.67556727	5327.458	28381807	-0.00035	13.94749
27	60.99514563	5306.895	28163134	-0.00039	11.40095
28	61.06769369	5269.131	27763743	0.057205	11.99061
29	60.53163694	5229.335	27345941	-0.01111	11.5717
30	61.9119398	5216.336	27210165	0.060423	11.99343
31	40.51748571	3546.745	12579403	-0.06772	11.91995
32	40.34997751	3489.868	12179180	-0.00521	11.68117
33	41.30509674	3598.124	12946496	-0.007	10.52229
34	40.56409096	3528.868	12452909	0.061434	11.64248
35	39.59282941	3516.395	12365032	-0.11815	12.01545
36	-24.72182183	1412.449	1995012	-0.27049	11.68998
37	-24.00880167	1408.917	1985047	-0.20272	11.09286
38	-25.28539507	1350.78	1824606	-0.07341	8.716199
39	-25.8549331	1410.029	1988182	-0.16327	11.46891

5.2.2 Feature Reduction

The features which are extracted in the feature extraction phase are then reduced to a few features which are further used for classification. This is done in order to reduce the dimensionality, redundancy and computational load.

Table 5.13: Value of FDR ratio calculated for each feature.

S. No.	Feature Name	Normal- Diastolic	Normal- Systolic	Systolic-Diastolic
1	Peak frequency	0.0723	0.7500	0.4124
2	Peak amplitude	0.7842	2.1565	0.4112
3	Total power	0.7380	1.2454	0.0022
4	THD	0.0005	0.0099	0.0054
5	IMD	0.0250	0.0444	0.0004
6	Peak frequency(s)	0.0296	0.3697	0.2898
7	BW(s)	0.0629	0.0726	0.0006
8	Q-factor(s)	0.0032	0.1813	0.4070
9	Peak frequency(p)	0.1505	1.0069	0.2560
10	BW(p)	0.0030	0.4201	0.1777
11	Q-factor(p)	0.1344	0.0016	0.0873
12	Ta	0.0707	13.1090	17.2189
13	Tb	5.9862	0.5120	3.5765
14	Crest factor	3.0335	7.1205	0.8307
15	Dynamic range	0.3169	0.2024	0.0448
16	Mean	0.0069	0.7351	0.4057
17	Standard deviation	1.1625	5.0208	0.3916
18	Variance	0.5692	3.7731	0.2592
19	Skewness	0.0063	0.0004	0.1474
20	Kurtosis	1.5198	1.7497	0.3642
21	ZCR	2.0339	2.1383	0.0122
22	RMS	1.1625	5.0208	0.3916
23	RMS1	0.4519	5.6353	4.8869
24	Max1	0.2117	9.9879	9.4525
25	ZCR1	2.1683	2.6070	0.1518
26	RMS2	1.2155	0.2682	1.0225
27	Max2	1.9291	0.0715	1.8384
28	ZCR2	2.4815	2.2341	0.1007

The features have been reduced using FDR and those features have been selected with higher FDR value. Table 5.13 shows the value of FDR calculated for all the features. As seen in table 5.14, Max1 has been selected as it has higher FDR value but skewness has not been selected due to its lower FDR value. After selection out of the total feature, only 7 features have been selected.

Table 5.14: List of features that were selected for classification.

S. No.	**Feature Name**
1	RMS1
2	RMS2
3	Ta
4	Tb
5	Kurtosis
6	Max1
7	Max2

5.2.3 Classification

The classification is done using the set of selected feature values. The feature set is divided into training set consisting of 96 signals and test set consisting of 50 signals. The classifiers are first trained using the training set and are then tested on the test set. The accuracy is then calculated according to how many test signals are classified correctly.

Using ANN as a classifier

Training and testing of neural network is done using Neural Network toolbox (nntool) in MATLAB. ANN used have input (7 neurons), hidden layer and an output layer (3 neurons). *Feed-forward Backpropagation* neural network has been used with *trainlm* as the training function. MSE (mean square error) has been chosen as the performance function. *Logsig* has been used as the tranfer function. First the neural network is trained using the training set consisting 94 samples. Then the trained network is simulated for 50 test samples. The neurons in the hidden layer have been varied from 2 to 7 neurons. The best accuracy has been achieved when the hidden layer has 5 neurons. 5 fold cross validation has been used and the result for each validation has been shown in figures 5.5 to 5.9 (for ANN with 5 neurons in hidden layer). These figures show the confusion matrix for each validation. The overall accuracy has been calculated by averaging out these 5 validation accuracies which comes out to be 98.8%.

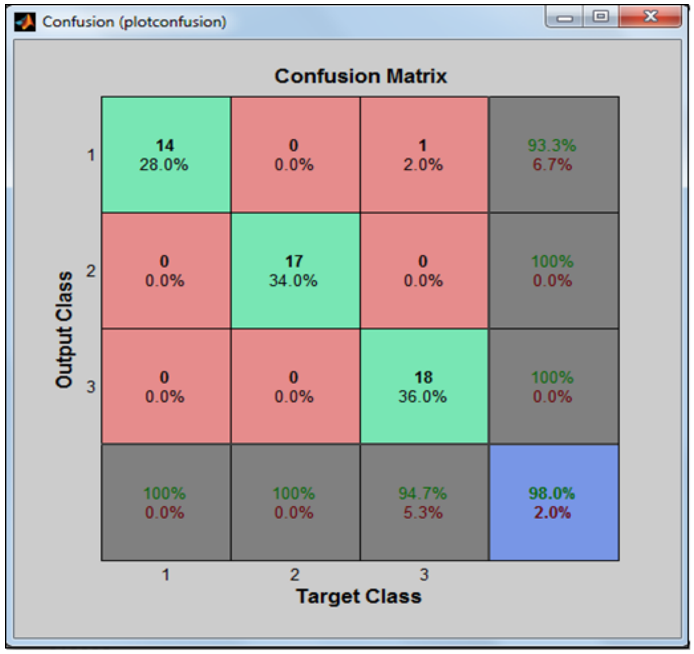

Figure 5.5: Confusion matrix for ANN as a classifier with 5 neurons in hidden layer (Result 1).

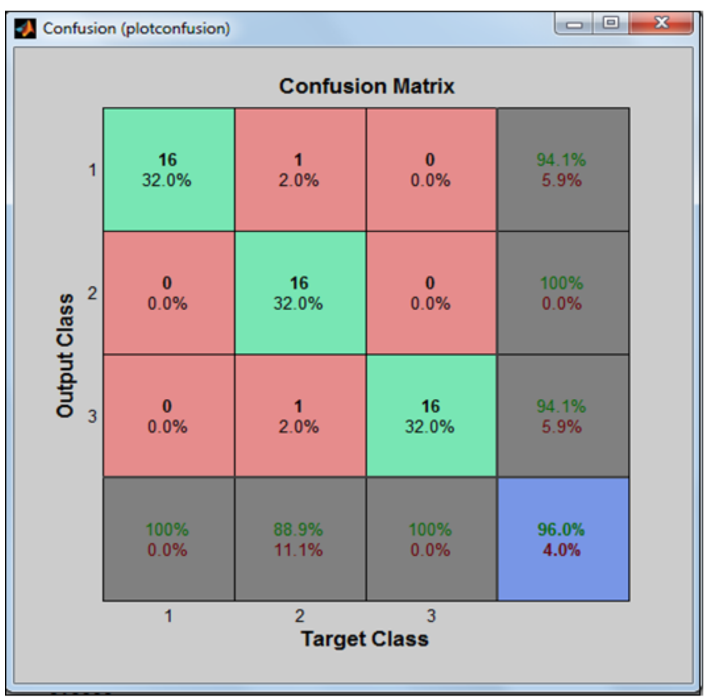

Figure 5.6: Confusion matrix for ANN as a classifier with 5 neurons in hidden layer (Result 2).

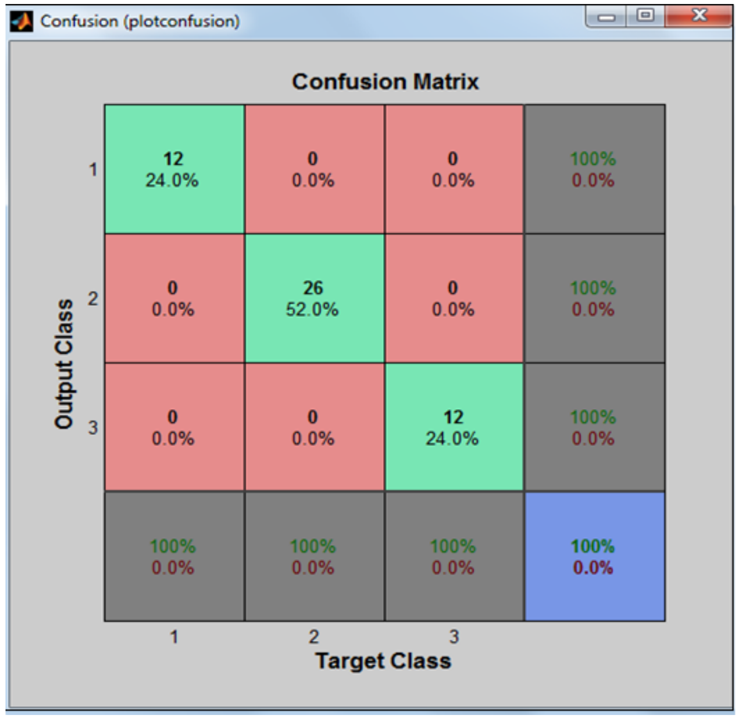

Figure 5.7: Confusion matrix for ANN as a classifier with 5 neurons in hidden layer (Result 3).

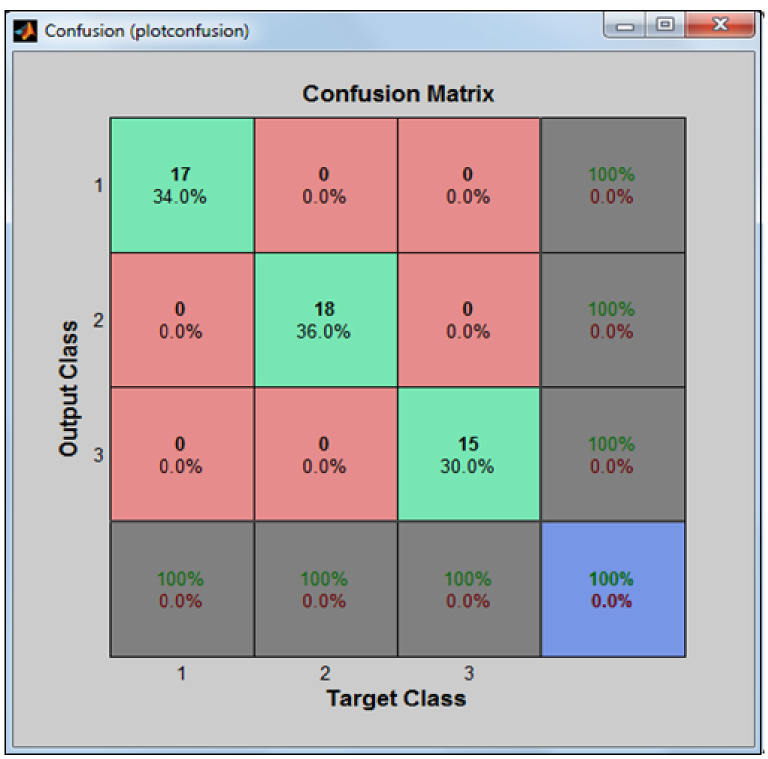

Figure 5.8: Confusion matrix for ANN as a classifier with 5 neurons in hidden layer (Result 4).

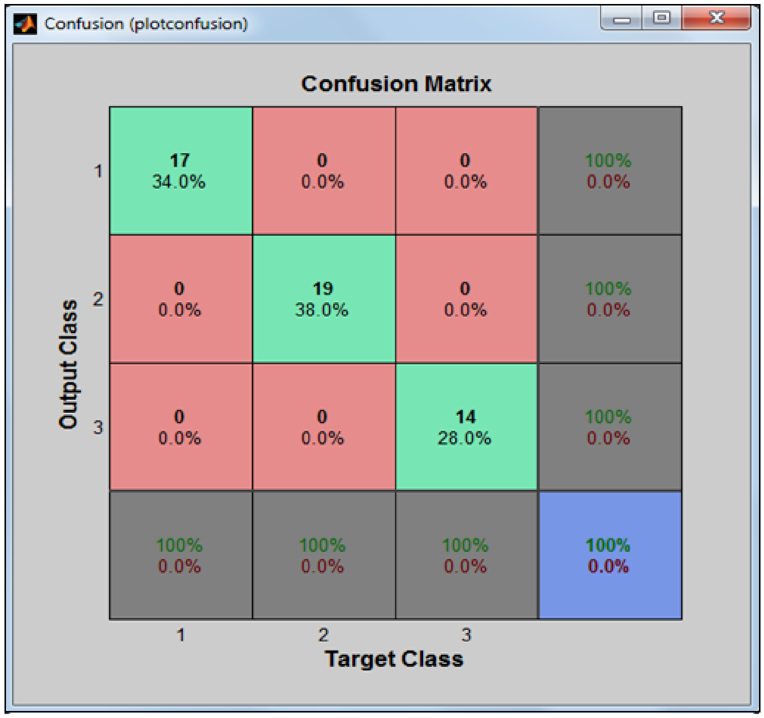

Figure 5.9: Confusion matrix for ANN as a classifier with 5 neurons in hidden layer (Result 5).

Using k-NN as a classifier

The k-NN has been used as a second classifier to classify the signals into pre-defined classes. The signals have been divided into test set (50 signals) and training set (96 signals). As shown in table 5.15, value of k is varied from 3 to 10 and accuracy was calculated. 5 fold cross-validation has been used to calculate the final accuracy.

Table 5.15: Accuracies using k-NN as a classifier.

k	Accuracy 1 (%)	Accuracy 2 (%)	Accuracy 3 (%)	Accuracy 4 (%)	Accuracy 5 (%)	Average Accuracy (%)
3	100	98	98	100	96	98.4
4	100	100	100	98	100	99.6
5	100	96	100	98	100	98.8
6	100	100	98	96	98	98.4
7	98	98	100	98	100	98.8
8	98	98	98	100	100	98.8
9	98	98	98	100	96	98
10	98	100	98	98	100	98.8

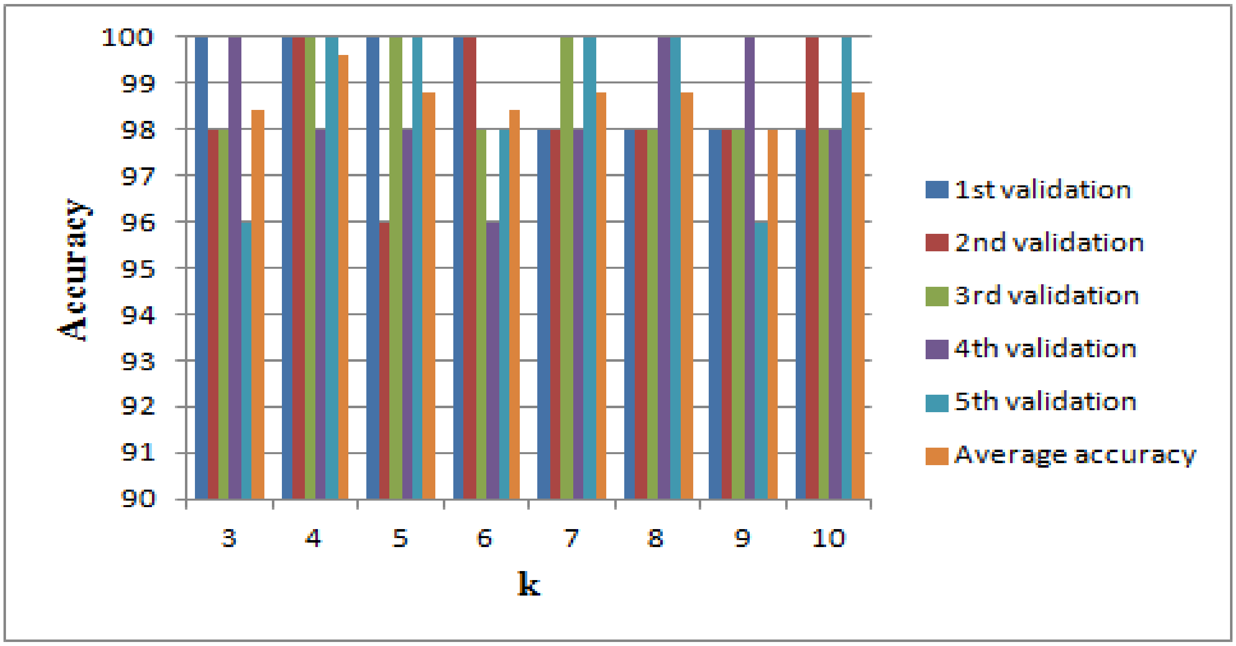

Figure 5.10: 5 fold validation and average accuracy using k-NN as a classifier.

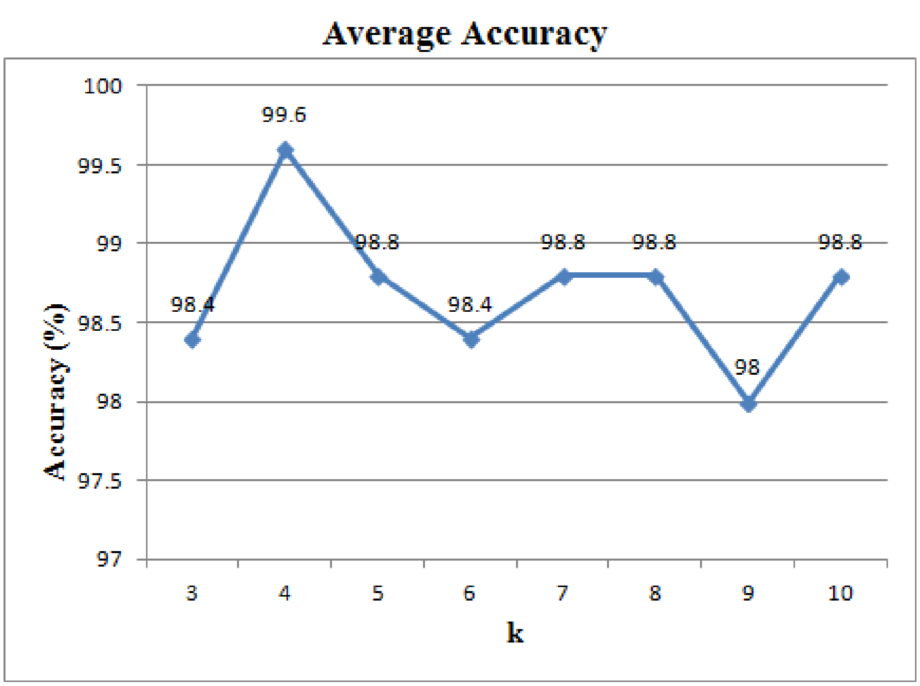

Figure 5.11: Average accuracy for different values of k using k-NN as a classifier.

Figure 5.10 shows the 5 validation accuracies and the average accuracy for each value of k. The average accuracy for all values of k has been plotted as shown in figure 5.11. From this figure it can be seen that highest average accuracy of 99.6% is achieved at k=4.

Using Fuzzy k-NN as a classifier

The Fuzzy k-NN has been used as a third classifier to classify the signals into pre-defined classes. The signals have been divided into test set (50 signals) and training set (96 signals). As shown in table 5.16, value of k is varied from 3 to 10 and accuracy is calculated. 5 fold cross-validation has been used to calculate the final accuracy.

Table 5.16: Accuracies using Fuzzy k-NN as a classifier.

k	Accuracy 1 (%)	Accuracy 2 (%)	Accuracy 3 (%)	Accuracy 4 (%)	Accuracy 5 (%)	Average Accuracy (%)
3	100	100	98	100	100	99.6
4	98	100	100	100	100	99.6
5	100	98	98	100	100	99.2
6	98	100	98	100	98	98.8
7	100	100	100	100	96	99.2
8	98	100	98	100	100	99.2
9	100	98	100	98	98	98.8
10	100	100	100	98	98	99.2

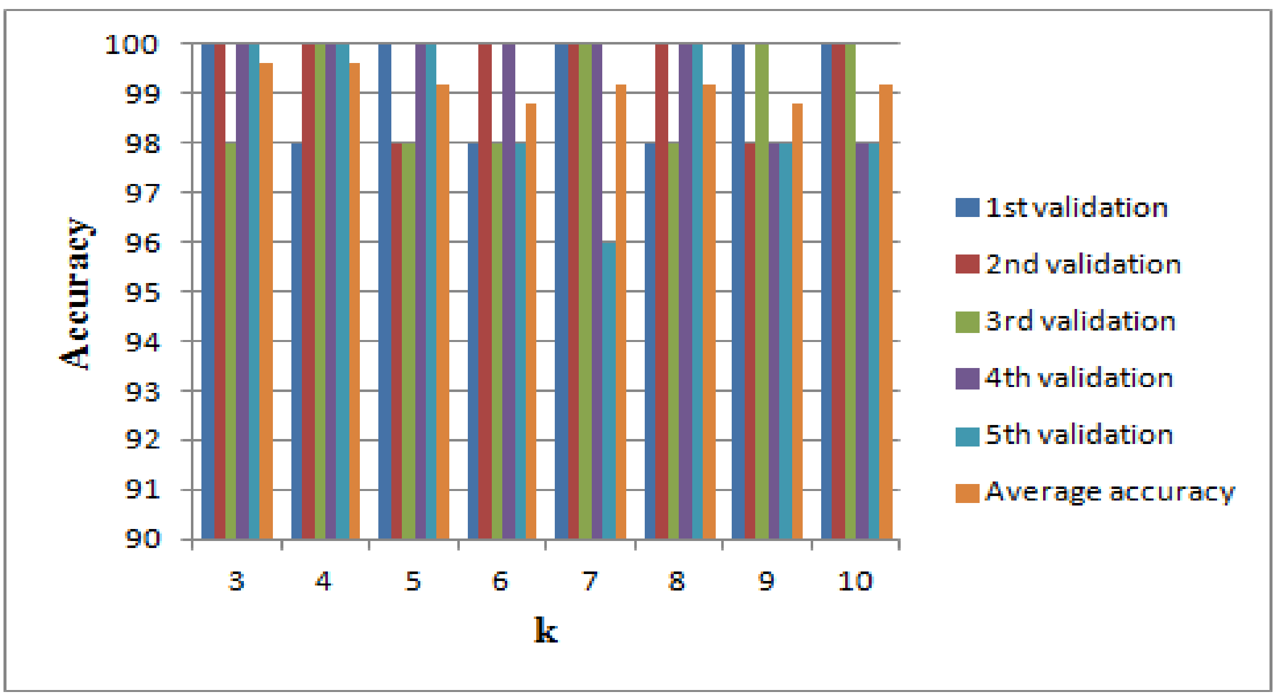

Figure 5.12: 5 fold validation and average accuracy using fuzzy k-NN as a classifier.

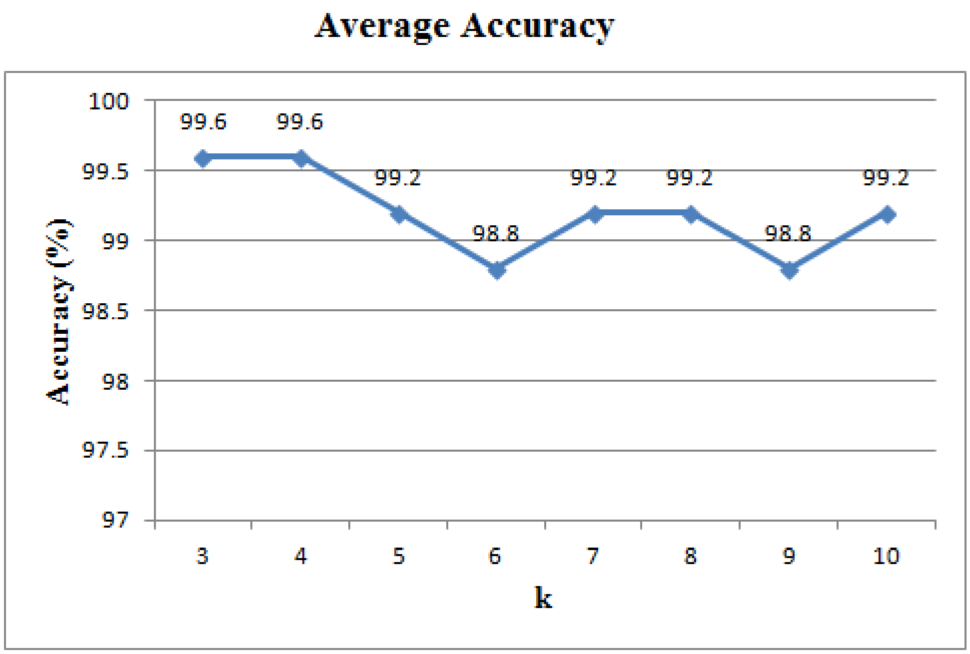

Figure 5.13: Average accuracy for different values of k using Fuzzy k-NN as a classifier.

Figure 5.12 shows the 5 validation accuracies and the average accuracy for each value of k. The average accuracy for all values of k has been plotted as shown in figure 5.11. From this figure it can be seen that highest average accuracy of 99.6% is achieved at k=3 and 4.

5.3 Classification of PCG signals using Adaptive Weighted FDR Algorithm

The features used for classifying the signals into their respective classes have been selected according to the FDR values calculated as shown in table 5.13. The selected features are shown in table 5.17.

Table 5.17: Selected features and their FDR weight value.

S. No.	Feature Name	FDR value (Normal-Diastolic)	FDR weight = FDR/T
1	ZCR	2.0339	0.18
2	Crest factor	3.0335	0.27
3	Kurtosis	1.5198	0.14
4	ZCR1	2.1683	0.19
5	ZCR2	2.4815	0.22
		Total (T) = 11.237	Total = 1

The adaptive weighted FDR algorithm has been developed in MATLAB [59]. The test samples are given as input first and classification is done according to the algorithm. The output of the algorithm is the class of the signal. Accuracy is calculated and confusion matrix has also been made according to the classification of test samples. An accuracy of 96% is achieved using this algorithm.

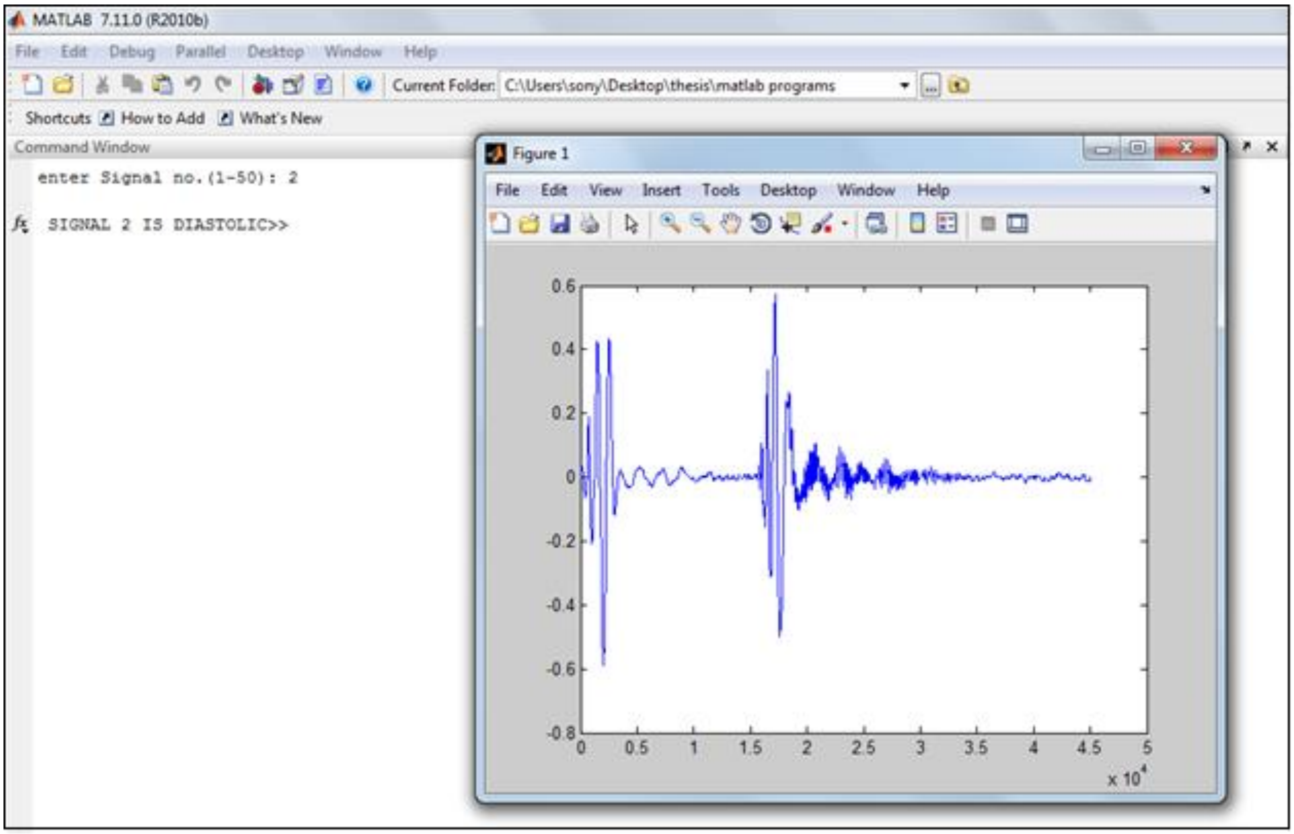

Figure 5.14: Classification of Diastolic murmur signal.

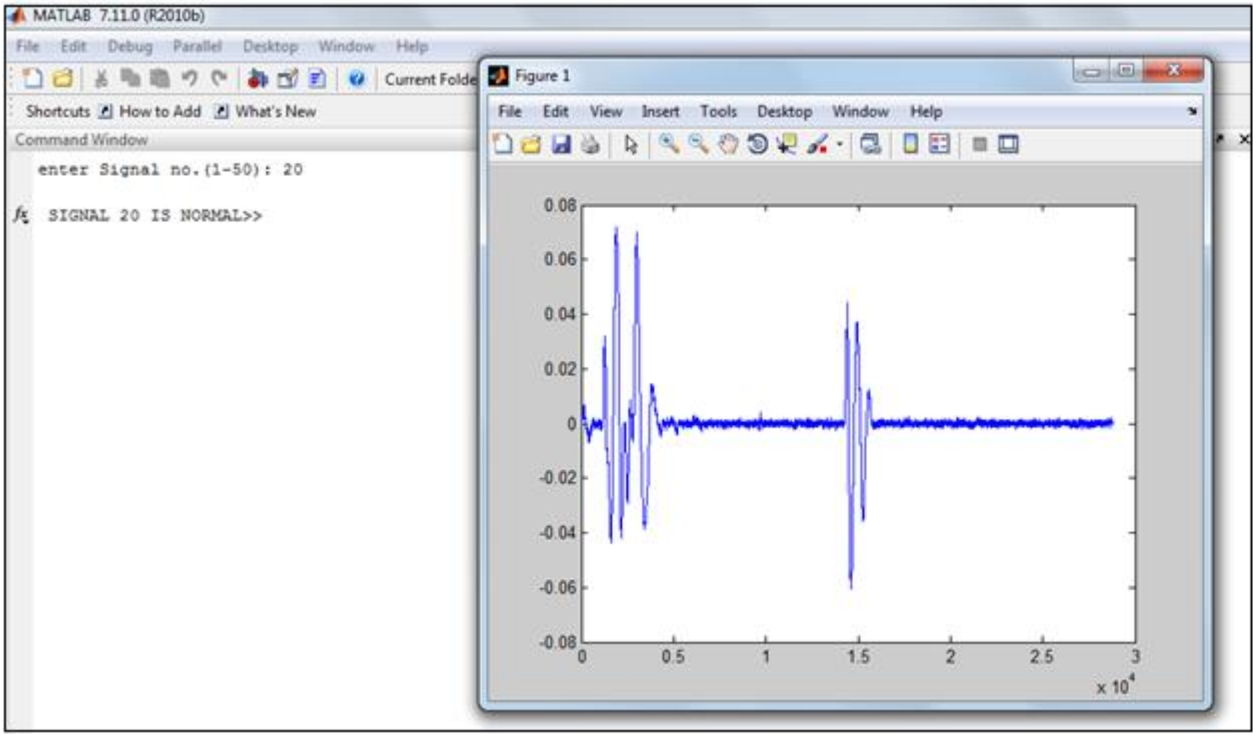

Figure 5.15: Classification of Normal signal.

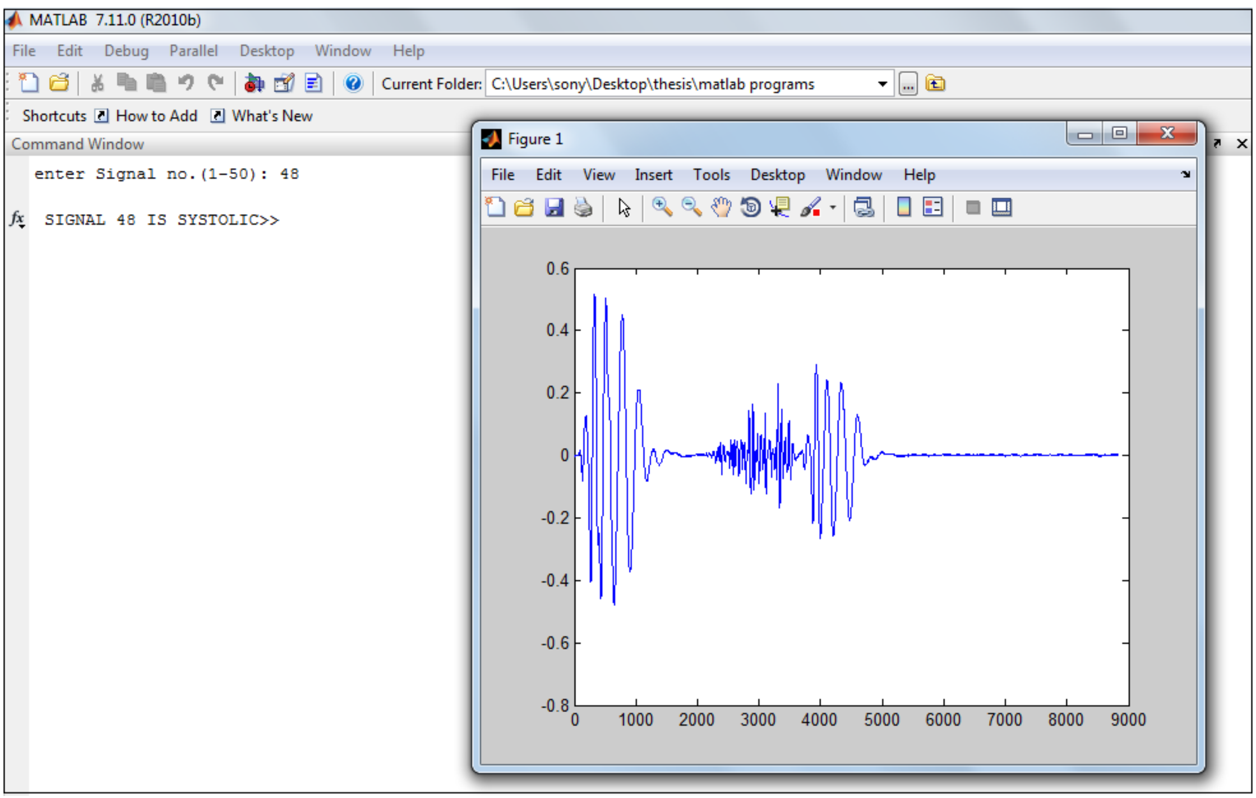

Figure 5.16: Classification of Systolic murmur signal.

Confusion matrix

Confusion matrix is the visualization of the performance of an algorithm. This matrix is also known as error matrix. Each column of the matrix represents the instances in a predicted class, while each row represents the instances in an actual class. In this confusion matrix as shown in figure 5.17, out of the 22 normal signals 21 have been classified correctly and 1 normal signal has been classified wrongly as diastolic murmur signal. Out of 13 systolic murmur signals, 12 have been classified correctly as systolic murmur signals and 1 systolic murmur signal has been classified as diastolic murmur signal. All the 15 diastolic murmur signals have been classified correctly.

PREDICTED

ACTUAL

Class	**NORMAL**	**SYSTOLIC**	**DIASTOLIC**
NORMAL	21	0	1
SYSTOLIC	0	12	1
DIASTOLIC	0	0	15

Figure 5.17: Confusion matrix for classification using Adaptive weighted FDR algorithm.

Out of all the classifiers used k-NN and Fuzzy k-NN has achieved marginally higher accuracy of 99.8% as compared to 98.8% using ANN with 5 neurons in hidden layer. For k-NN the highest accuracy has been achieved at k=4. For fuzzy k-NN highest accuracy has been achieved at k=3 and 4. For these 3 classifiers 5 fold cross-validation has been used. The adaptive weighted FDR algorithm achieved an accuracy of 96%.

CHAPTER 6

CONCLUSION AND FUTURE SCOPE

6.1 Conclusion

PCG signals are capable of indicating the heart problem at an earlier stage which can be very useful in preventing fatality due to heart problems. Research in this area can be very helpful for easy and earlier diagnosis of various heart diseases.

In this thesis the PCG signal has been studied and has been classified into three classes, namely normal signal, systolic murmur signal, diastolic murmur signal. Many features in time, frequency and statistical domains have been extracted and the best features are selected for the classification using FDR. Various classifiers have been used for classification and the best accuracy of 99.6% has been achieved using both k-NN and fuzzy k-NN.

Two new features, Max1 and Max2, have also been proposed in this study for classification of the PCG signals.

Also, adaptive weighted FDR algorithm has also been developed in MATLAB to classify the PCG signals into pre-defined classes. An accuracy of 96% has been achieved using this algorithm.

6.2 Future Scope

Hybrid classifier can also be implemented dataset can be increased for classification of PCG signals with higher accuracy.

The proposed method can be implemented in electronic stethoscopes which can be used for detecting any abnormalities at an earlier stage.

The case of continuous murmur signal has not been included in this study. It can also be included for classification in further studies.

REFERENCES

[1] D. Prakash, T. Uma Mageshwari, K. Prabakaran and A. Suguna. "Detection of Heart Diseases by Mathematical Artificial Intelligence Algorithm Using Phonocardiogram Signals". *International Journal of Innovation and Applied Studies*, vol. 3, No. 1, 2013

[2] Z. Jiang and S. Choi. "A cardiac sound characteristic waveform method for in-home heart disorder monitoring with electric stethoscope". *Expert Systems with Applications*, vol. 31, pp 286-298, 2006

[3] L. Cromwell, F.J. Weibell and E.A. Pfeiffer. *"Biomedical Instrumentation and Measurements*" Pearson Education, Second Edition, 2010

[4] V. Nigam and R. Priemer. "A simplicity-based fuzzy clustering approach for detection and extraction of murmurs from the phonocardiogram". *IOP publishing physiological measurement*, vol. 29, pp. 33–47, 2008

[5] http://www.learntheheart.com/cardiology-review/heart-murmurs/

[6] http://www.worldinvisible.com/apologet/humbody/heart.htm

[7] http://www.innerbody.com/image/card01.html

[8] http://www.nottingham.ac.uk/nursing/practice/resources/cardiology/function/conduction.php

[9] http://www.bostonscientific.com/lifebeat-online/heart-smart/electrical-system.html

[10] http://www.wonderwhizkids.com/index.php/heart

[11] http://learnpediatrics.com

[12] http://www.nlm.nih.gov/medlineplus/ency/imagepages/19613.htm

[13] http://www.learntheheart.com/cardiology-review/describing-murmurs/

[14] https://www.nhlbi.nih.gov/health/health-topics/topics/heartmurmur/causes.html

[15] http://www.aafp.org/afp/2000/0601/p3343.html

[16] D. Barschdorff, U. Femmer and E. Trowitzsch. “Automatic phonocardiogram signal analysis in infants based on wavelet transforms and artificial neural networks” *Computers in Cardiology 1995*, pp. 753-756, 1995

[17] I. Kim, S. M. Lee, H. S. Yeo, W. T. Han, and S. H. Hong. “Feature extraction for heart sound recognition based on time-frequency analysis” *BMES/EMBS Conference, 1999. Proceedings of the First Joint*. vol. 2, 1999

[18] T. Olmez and Z. Dokur, “Classification of heart sounds using an artificial neural network”. *Pattern Recognition Letters*, vol. 24, pp. 617-629, 2003

[19] A. Voss, A. Mix, and T. Hübner. “Diagnosing Aortic Valve Stenosis by Parameter Extraction of Heart Sound Signals”, *Annals of Biomedical Engineering*, vol. 33, pp. 1167-1174, 2005

[20] Z. Dokur and T. Ölmez. "Heart sound classification using wavelet transform and incremental self-organizing map." *Digital Signal Processing*, vol.18, pp. 951-959, 2008

[21] S. Babaei and A. Geranmayeh. “Heart sound reproduction based on neural network classification of cardiac valve disorders using wavelet transforms of PCG signals” *Computers in Biology and Medicine* vol. 39, pp. 8-15, 2009

[22] Y. Chen, S. Wang, C.H. Shen, and F. Choy. "Intelligent identification of childhood musical murmurs." *Journal of Healthcare Engineering*, vol. 3, pp. 125-140, 2012

[23] M. Guermoui, M. L. Mekhalf and K. Ferroudji “Heart sounds analysis using wavelets responses and support vector machines.” *8th International Workshop on Systems, Signal Processing and their Applications (WoSSPA)*, pp. 233-238, 2013

[24] H. Shino, H. Yoshida, K. Yana, K. Harada, J. Sudoh and E. Harasewa. “Detection and classification of systolic murmur for phonocardiogram screening." *Engineering in Medicine and Biology Society, 1996. Bridging Disciplines for Biomedicine. Proceedings of the 18th Annual International Conference of the IEEE*, vol. 1, 1996

[25] S.A. Pavlopoulos, A. CH Stasis and E.N. Loukis. "A decision tree–based method for the differential diagnosis of Aortic Stenosis from Mitral Regurgitation using heart sounds." *Biomedical engineering online*, vol. 3, 2004

[26] T. S. Leung, P. R. White, W. B. Collis, E. Brown and A. P. Salmon. "Classification of heart sounds using time-frequency method and artificial neural networks." *Engineering in Medicine and Biology Society, 2000. Proceedings of the 22nd Annual International Conference of the IEEE*. vol. 2. pp. 988-991, 2000

[27] Z. Sharif, M.S. Zainal, A.Z.S. Ameri, and S.H.S. Salleh. "Analysis and classification of heart sounds and murmurs based on the instantaneous energy and frequency estimations." *TENCON 2000. Proceedings*, vol. 2, pp.130-134, 2000

[28] R. Amarnath, J. Muruganantham, K.V. Jawahar, C. Ka1yanasundaram. "Methods for classification of phonocardiogram," *TENCON 2003. Conference on Convergent Technologies for the Asia-Pacific Region*, vol.4, pp.1514-1515, Oct. 2003

[29] M. El-Segaier, O. Lilja, S. Lukkarinen, Leif Sörnmo, R. Sepponen and E. Pesonen. "Computer based detection and analysis of Heart Sound and Murmur." *Annals of Biomedical Engineering*, vol. 33, pp. 937-942, 2005

[30] A.L. Noponen S. Lukkarinen, A. Angerla, and R. Sepponen. "Phono-spectrographic analysis of heart murmur in children." *BioMed Central, BMC Pediatrics*, vol. 7, 2007

[31] V. Nigam and R. Priemer "A simplicity-based fuzzy clustering approach for detection and extraction of murmurs from the phonocardiogram", *IOP publishing physiological measurement*, vol. 29, pp. 33–47, 2008

[32] E. Delgado-Trejos, A. F. Quiceno-Manrique, J. I. Godino-Llorente, M. Blanco-Velasco, and G. Castellanos-Dominguez. "Digital Auscultation Analysis for Heart Murmur Detection." *Annals of Biomedical Engineering*, vol. 37, pp. 337-353, Feb 2009

[33] J. Vepa, "Classification of heart murmurs using cepstral features and support vector machines", *31st Annual International Conference of the IEEE EMBS*, Minneapolis, Minnesota, USA, Sept 2009

[34] I. Maglogiannis, E. Loukis, E. Zafiropoulos and A. Stasis. "Support Vectors Machine-based identification of heart valve diseases using heart sounds", *Computer methods and programs in biomedicine*, vol. 95, pp. 47-61, 2009

[35] S. Ari, K. Hembram and G. Saha. "Detection of cardiac abnormality from PCG signal using LMS based least square SVM classifier", *Expert Systems with Applications*, vol. 37, pp. 8019-8026, 2010

[36] S. Choi and Z. Jiang. "Cardiac sound murmurs classification with autoregressive spectral analysis and multi-support vector machine technique", *Computers in Biology and Medicine*, vol. 40, pp. 8–20, 2010

[37] L. H. Cherif, S. M. Debbal and F. Bereksi-Reguig. "Choice of the wavelet analyzing in the phonocardiogram signal analysis using the discrete and the packet wavelet transform", *Expert Systems with Applications*, vol. 37, pp. 913–918, 2010

[38] S. Yuenyong, A. Nishihara, W. Kongprawechnon and K. Tungpimolrut. "A framework for automatic heart sound analysis without segmentation." *BioMedical Engineering OnLine*, vol. 10, pp.10-13, 2011

[39] S. Sanei, M. Ghodsi and H. Hassani. "An adaptive singular spectrum analysis approach to murmur detection from heart sounds." *Medical Engineering & Physics*, vol. 33, pp.362–367, 2011

[40] M.A. Akbari, K. Hassani, J. D. Doyle, M. Navidbakhsh, M. Sangargir, K. Bajelani and Z. S. Ahmadi. "Digital Subtraction Phonocardiography (DSP) applied to the detection and characterization of heart murmurs", *BioMedical Engineering OnLine*, vol. 10, pp.1-14, 2011

[41] M.A. Akbari, K. Hassani, John D. Doyle, M. Navidbakhsh, M. Sangargir, K. Bajelani and M. Foroughi. "Separating the random murmur component of the phonocardiogram from the underlying deterministic heart sounds applied to Digital Subtraction Phonocardiography (DSP)" *18th Iranian Conference on BioMedical Engineering (ICBME)*, 2011

[42] R. R. Sarbandi, R. Ramezani, J. D. Doyle, M. Navidbakhsh, K. Hassani and H. Torabiyan. "A color spectrographic phonocardiography (CSP) applied to the detection and characterization of heart murmurs: preliminary results". *BioMedical Engineering OnLine*, vol. 10, 2011

[43] H. Xiao-Juan, Z. Jia-Wei, C. Gui-Tao, Z. Hong-Hai and L. Hao. "Feature extraction and choice in PCG based on Hilbert Transfer." *4th International Congress on Image and Signal Processing*, 2011

[44] S.M. Debbal and F. Bereksi-Reguig "Detection of Differences of the Phonocardiogram Signals by Using the Continuous Wavelet Transform Method", *Biomedical Soft Computing and Human Sciences*, vol. 18, pp. 73-81, 2012

[45] F. Safara, S. Doraisamy, A. Azman, A. Jantan and S. Ranga. "Wavelet Packet Entropy for Heart Murmur Classification" *Hindawi Publishing Corporation*, Advances in Bioinformatics, 2012

[46] H. Uguz "Adaptive neuro-fuzzy inference system for diagnosis of the heart valve diseases using wavelet transform with entropy", *Neural Comput & Applic*, vol. 21, pp. 1617-1628, 2012

[47] Y. Chen, S. Wang, Chia-Hsuan Shen, and F. K. Choy. "Matrix decomposition based feature extraction for murmur classification", *Medical Engineering & Physics*, vol. 34, pp. 756– 761, 2012

[48] H. Sun, W. Chen and J. Gong. "An Improved Empirical Mode Decomposition-Wavelet Algorithm for Phonocardiogram Signal Denoising and its Application in the First and Second Heart Sound Extraction." *6th International Conference on Biomedical Engineering and Informatics (BMEI 2013)*, 2013

[49] F. Safara, S. Doraisamy, A. Azman, A. Jantan and A. R. A. Ramaiah. "Multi-level basis selection of wavelet packet decomposition tree for heart sound classification" *Computers in Biology and Medicine*, vol. 43, pp.1407-1414, 2013

[50] M. Singh and A. Cheema. "Heart Sounds Classification using Feature Extraction of Phonocardiography Signal" *International Journal of Computer Applications*, vol. 77, pp. 13-17, 2013

[51]S. Patidar and R. B. Pachori. "Classification of cardiac sound signals using constrained tunable-Q wavelet transform." *Expert Systems with Applications*, vol. 41, pp. 7161-7170, 2014

[52] F. Safara, S. Doraisamy, A. Azman, A. Jantan and S. Ranga. “Diagnosis of Heart Valve Disorders through Trapezoidal Features and Hybrid Classifier.” *International Journal of Bioscience, Biochemistry and Bioinformatics*, vol. 3, 2013

[53] P.J. Bentley, G. Nordehn, M. Coimbra and S. Mannor. “The PASCAL Cassifying Heart Sounds Challenge” 2011, available at http://www.peterjbentley.com/heartchallenge/index.html

[54] E. M. Brown, T.S. Leung, W.B. Collis and A.P. Salmon. “Heart Sounds Made Easy”, Elsevier, Second Edition, 2008

[55] G. Amit, N. Gavriely and N. Intrator. “Cluster analysis and Classification of Heart Sounds.” *Biomedical Signal Processing and Control,* vol. 4, pp. 26-36, 2009

[56] Rabiner L, and Shafer R. Digital Processing of Speech Signals. 2nd ed., Prentice Hall: New Jersey, USA, 2008

[57] http://www.odec.ca/projects/2006/stag6m2/background.html

[58] https://en.wikipedia.org/wiki/K-nearest_neighbors_algorithm

[59] M. Singh, S. Singh and S. Gupta. "An information fusion based method for liver classification using texture analysis of ultrasound images." *Information Fusion,* vol. 19, pp. 91-96, 2014